Since January 2020 Elsevier has created a COVID-19 resource centre with free information in English and Mandarin on the novel coronavirus COVID-19. The COVID-19 resource centre is hosted on Elsevier Connect, the company's public news and information website.

Trends in Analytical Chemistry 144 (2021) 116424

Contents lists available at ScienceDirect

Trends in Analytical Chemistry

journal homepage: www.elsevier.com/locate/trac

Paper-based analytical devices for virus detection: Recent strategies for current and future pandemics

Tugba Ozer [a], Charles S. Henry [b, c, *]

[a] Yildiz Technical University, Faculty of Chemical-Metallurgical Engineering, Department of Bioengineering, 34220, Istanbul, Turkey
[b] Colorado State University, Department of Chemistry, Fort Collins, CO, 80523, USA
[c] Colorado State University, School of Biomedical Engineering, Fort Collins, CO, 80523, USA

ARTICLE INFO

Article history:
Available online 26 August 2021

Keywords:
Paper-based
Virus detection
COVID-19
SARS-CoV-2
Point of care
Infectious diseases
Optical
Electrochemical
Nanomaterials

ABSTRACT

The importance of user-friendly, inexpensive, sensitive, and selective detection of viruses has been highlighted again due to the recent Coronavirus disease 2019 (COVID-19) pandemic. Among the analytical tools, paper-based devices (PADs) have become a leading alternative for point-of-care (POC) testing. In this review, we discuss the recent development strategies and applications in nucleic acid-based, antibody/antigen-based and other affinity-based PADs using optical and electrochemical detection methods for sensing viruses. In addition, advantages and drawbacks of presented PADs are identified. Current state and insights towards future perspectives are presented regarding developing POC diagnosis platform for COVID-19. This review considers state-of-the-art technologies for further development and improvement in PADs performance for virus detection.

1. Introduction

Viruses can cause serious diseases including rabies [1], dengue [2], hepatitis [3], Ebola [4], AIDS [5], avian influenza [6], SARS, MERS, etc. [7]. Viral load can have a great impact on the severity of the diseases [8]. In addition to acute diseases, some viruses, such as hepatitis B and C, can lead to chronic infections or cancer [9]. Viruses are spread by infected carriers, contact with contaminated surfaces, and exposure to aerosolized virus particles [10,11]. Viral infections are currently responsible of one third of the deaths annually worldwide [12]. Recently, the severe acute respiratory syndrome coronavirus 2 (SARS-CoV-2 virus) has caused a pandemic leading to millions of deaths and a huge economic crisis around the world [13].

There are more than 1500 identified human and animal viruses to date, exhibiting wide variety in structure, composition and genome [14]. Viruses include single- or double stranded RNA and DNA variants and have an outer protein called the capsid which consists of one or more structural proteins, surrounding the viral genome [15]. The nucleocapsid, which is composed of the genome along with the nucleic acid-associated proteins, can also be surrounded by an envelope in some virus families. The envelope consists of glycoproteins and glycosylated-membrane proteins that takes the form of spikes or knobs. Viruses can be classified based on the replication strategies of their genomes. Also, they can be separated into different categories according to their shape as enveloped, filamentous, icosahedral, or head-and-tail viruses. Enveloped viruses such as avian influenza viruses, SARS Coronavirus-1 (SARS-CoV), Ebola virus, Zika virus, Middle East respiratory syndrome-related coronavirus (MERS-CoV), and SARS-CoV-2 have caused outbreaks so far [16–18]. A recent global outbreak, SARS-CoV-2, spread rapidly, affecting hundreds of millions of people and was deemed a pandemic by the World Health Organization [19,20].

Various respiratory infections are caused by coronaviruses, SARS-CoV, and MERS Coronavirus (MERS), and can be transmitted through animals to humans [21]. Although the spread of COVID-19 is faster than former coronavirus infections, global mortality rate is 6%, less than SARS-CoV (10%) and MERS-CoV (35%) [22]. The protein components of SARS-CoV-2 include the spike glycoprotein, envelope proteins, and matrix and nucleocapsid proteins [23]. The spike protein is the most abundant transmembrane protein, showing

* Corresponding author. Colorado State University, Department of Chemistry, School of Biomedical Engineering, Fort Collins, CO, 80523, USA.
E-mail address: Chuck.Henry@colostate.edu (C.S. Henry).

https://doi.org/10.1016/j.trac.2021.116424
0165-9936/

high immunogenicity. SARS-CoV-2 can be distinguished from other coronaviruses through nucleic acid sequence that produces the protein sequence. The nucleocapsid protein (also called the N protein), which is a structural protein, is responsible for the viral replication cycle [24]. To diagnose COVID-19, S and N proteins have been used as the most valuable antigen biomarkers [25]. In addition, Immunoglobulins IgG, IgM, and IgA are generated in response to SARS-CoV-2 infections starting on the fourth to seventh days of the disease have been used to detect current or previous SARS-CoV-2 in recent studies [26].

Coronavirus disease 2019 (COVID-19) is the infectious disease which is caused by the SARS-CoV-2 virus. While COVID-19 is a current focus, many other viruses are also of significant concern. Influenza, which targets the respiratory system, is considered to be the most common infectious disease, causing three pandemics in twentieth century alone [27]. Due to the high risk of transmission and epidemics/pandemics, it is important to rapidly detect influenza infections. The human immunodeficiency virus (HIV), which is a retrovirus, is another important virus that causes immunodeficiency syndrome (AIDS), attacking the immune system [28]. Mortality can be reduced by early diagnosis and clinical treatment of the infection [29]. Human noroviruses (HuNoVs) are the leading cause of foodborne illnesses with around 21 million cases of acute gastroenteritis and $5.8 billion costs annually in the US [30]. HuNoVs have a wide range of genetic variation, resulting in at least nine genotypes of HuNoVs consisting of 150 strains. Among them, GII.4 is the most common genotype, which is responsible for about 80% of all norovirus outbreaks since 2002 [31]. Respiratory syncytial virus (RSV), which has a single-stranded negative-sense RNA encoding 11 proteins, lead to mild to moderate respiratory illnesses such as bronchiolitis and pneumonia, particularly in infants and elderly people [32]. Characteristics of RSV are similar to other viral respiratory infections with transmission through aerosols due to early symptoms including coughing and sneezing [33]. Zika virus, which is a flavivirus, is spread by mosquitoes. The virus causes congenital malformations and microcephaly during pregnancy, and neurologic complications such as neuropathy and Guillain-Barre syndrome [34]. Chikungunya and dengue viruses are both enveloped positive-stranded RNA genome arboviruses which cause epidemics in countries of Latin America and the Pacific [35]. These viruses are also transmitted by mosquitos and result in life threating infectious diseases [36]. According to WHO reports, no effective vaccines or antivirals are available for chikungunya virus [37]. Hepatitis B virus, which is a small DNA virus of the Hepanaviridae family, infects approximately two billion people worldwide every year [38]. This virus causes acute hepatitis, chronic hepatitis, cirrhosis, and hepatocellular carcinoma [39]. Porcine epidemic diarrhea virus (PEDV), which is a member of the coronavirus family, disrupts epithelial cells of the small intestine, resulting in an acute intestinal infectious disease in piglets and fattening pigs [18,40]. Pseudorabies virus (PRV), which is a neurotrophic alpha-herpes virus with a double-stranded DNA genome, infects swine and has several secondary hosts such as cattle, dogs, and cats [41]. The presence of PRV infection in humans causes respiratory distress and neurologic disorders and has been shown in recent reports [42]. To avoid pandemics and viral diseases, timely and sensitive detection of viruses become crucial for both developed and developing countries. The recent studies on developing PADs for detection of viruses are related to aforementioned viruses and they have been discussed in detail in applications section.

Viral separation, immunofluorescence-based on microscopy, enzyme-linked immunosorbent assays and nucleic acid amplification techniques such as polymerase chain reaction (PCR) are commonly used for viral detection [43]. Although these techniques are highly sensitive, they require laborious and time-consuming steps to be completed over days and, they rely on expensive reagents/equipment. Thus, it is necessary to develop rapid, low-cost sensing platforms for viral detection to control outbreaks in a timely manner. Paper-based analytical devices (PADs) were first used in the 17th century and have become popular due to their properties of biocompatibility, porosity, ease of modification, flexibility, chemically inertness, eco-friendly, and ease of storage and transportation [44,45]. Since the working principles of PADs are based on power-free fluid transport by capillary action, PADs are easily used with various sample types. When the Whitesides group introduced microfluidic patterns on a paper using a photoresist for fluidic control in 2007, a milestone was achieved for the development of microfluidic paper-based analytical devices (μPADs) [46]. The same group proposed a wax printing technology to create microfluidic patterns and various μPADs using colorimetric detection [47]. However, the assays and analytes were limited to chemical reactions that produce colored products. In 2009, the first electrochemical paper-based analytical device (ePAD) was develop by Henry group to overcome this issue and improve analytical performance of μPADs [48]. A review covering the first ten years of ePADs has recently been presented in Ref. [49].

Paper is less expensive than poly (ethylene terephthalate) and glass among other microfluidic substrates [50]. Although there are various paper substrates including chromatography paper, filter paper, office paper, cardboard, etc., filter paper has been the most used in the microfluidic sensor development [51]. Selection of paper type varies based on the desired hydrophilicity, pore size, and thickness, all of which impact the analytical performance of PADs. Paper has also been used in lateral flow assays (LFAs), dipsticks and microfluidic μPADs for applications including clinical, food, environmental, and healthcare monitoring [52]. PADs are suitable for point-of-care (POC) diagnosis of viral diseases, especially in developing countries confront with limited resources.

In this review, fabrication and detection methods of PADs for virus sensing are summarized and also, recent developments and applications from January 2020 to May 2021 are presented in detail. Moreover, challenges and future technologies are identified in conclusions and future prospects section.

2. Fabrication methods

Paper has been employed in LFAs, dipsticks, and μPADs [53]. According to the complexity of the application, two- (2D) or three-dimensional (3D) PADs can be fabricated. Specific regions of the cellulose paper are changed from hydrophilic to hydrophobic for both types of devices [54]. 2D- and 3D-PADs have been fabricated by wax printing [47], inkjet printing [55], photolithography [46], flexographic printing [56], plasma treatment [57], laser treatment [58], wet etching [59], ink stamping [60], lacquer spraying [61], and screen printing [62] on paper substrates. Since wax is inexpensive and non-toxic, wax printing has been more widely used to fabricate PADs compared to other methods. Alternatively, a desktop digital craft plotter/cutter and technical drawing pens have been introduced as low-cost PAD fabrication method [63]. PADs typically have regions assigned for sample introduction, liquid flow, and chemical or biochemical reactions [64]. Hydrophobic barriers are commonly to define channels control flow of analytes and reagents through microchannels, prevent leakage, and stop cross-contamination between multiplex assays.

LFAs are a type of 2D-PADs and were first reported in 1956 [65]. LFAs consist of a sample pad, a conjugate pad, a flow membrane (typically nitrocellulose) and an absorbent pad. The sample pad can be exploited for adjusting pH and/or pretreating the sample since it is the first region that sample contacts. Cellulose, glass fibre, Rayon and modified filtration substrates can be selected as sample pads to

properly deliver the sample to the conjugate pad, which is commonly made of glass fibre, polyester or rayon [66]. Generation of a signal at the test (T-line) and control (C-line) lines in LFAs depends on covalent or passive modification of the conjugate pad with labels such as gold [67], magnetic nanoparticles [68], fluorescence labels [69], quantum dots [70], carbon nanotubes [71], enzymes [72] and liposomes [73]. After the sample passes the conjugate pad, analyte is captured at the T-Line and excess antibody at the C-line. Nitrocellulose is typically used as the flow membrane due to the presence of charged nitro groups that help immobilize proteins [66]. Finally, the sample arrives to the absorbent pad which is used to wick the liquid for through the device. The materials used for absorbent pad are the same as the sample pad [74]. In addition, backing materials made of polystyrene, polyester or adhesive polymer and tape are used to maintain device integrity during the assay. LFAs have advantages such as long shelf-life (up to 1–2 years), low-cost (~USD 0.10–2), and the need of small volume of sample. The sensitivity can be improved by manipulating the membrane materials, reagents, and labels, and optimizing flow [75]. However, LFAs have some drawbacks in that their reproducibility is poor because of the variation of cellulose-based materials from batch-to-batch and, analytical or numerical models are not useful for prediction of flow in the porous membrane [53].

In addition to 2D-PADs, 3D-PADs allow liquid flow in X, Y, and Z directions by folding or stacking paper layers typically using double-sided adhesive tape. 3D-PADs differ from 2D-PADs with the use of multiple paper layer for the device assembly. The configuration of 3D-PADs provides precise time-control of the fluid flow and multiplex detection [64,76]. Also, it is possible to control incubation time of the target and integrate various components. For example, the Chailapakul group recently developed a pop-up paper device for detection of hepatitis B virus DNA [77]. The pop-up device includes a reagent zone, a sample zone, working, counter, and reference electrodes, and a conducting pad (Fig. 1A). The PAD was patterned using wax-printing. The counter and reference electrodes were printed on the front side of the PAD, and the working electrode on the back side of the PAD. After the sample zone was modified with (1S,2S)-2-aminocyclopentanecarboxylic acid (acpcPNA) probe, the device was cut and folded to generate a pop-up architecture. The fluidic path was able to be controlled due to the open and closed state of the device, allowing separation of reagent and detection zones. Using this design, contamination can be eliminated during washing since the target DNA is hybridized before hexacyanoferrate (III)/(II) is introduced to the reagent zone. Another 3D origami PAD was developed for detection of human immunodeficiency virus (HIV) by Chen et al. [78]. The 3D-PAD includes a strip, a detection pad, an indication pad, and three absorbent pads consisting of hydrophilic channels, wells, holes or hydrophobic zones generated by wax printing. Whereas 3D design was used to decrease manual operation steps and PAD size, a "timer" function was developed for indicating the timing of the ELISA steps. To initiate the timer, washing buffer is added to the detection wells. Then, the fluid is transported to the absorbent pads and the dye wells at a controlled flow rate. The signal is based on the solution turning green color in indication pad owing to its pretreated wells. The proposed configuration enables controlling of the time at which different steps are to be performed due to color formation. Fabrication methods for PADs with recent developments have been highlighted in Refs. [45,79–81].

3. Detection and signal read-out methods

Optical and electrochemical detection methods have been used for viral detection [15]. Optical detection is based on measuring optical signals such as fluorescence, chemiluminescence, and color generated due to binding of analytes with their probes. Colorimetric methods, which are based on colorimetric reactions between target analytes and chromogenic substances, are the most popular among optical methods due to their simplicity. Although fluorescence detection gives more sensitive detection among other methods, an excitation light source, fluorescent dyes, intrinsic fluorophores, and a detector are necessary to measure the emission intensity versus analyte concentrations, making the approach more complex compared to colorimetric methods. The signal generated

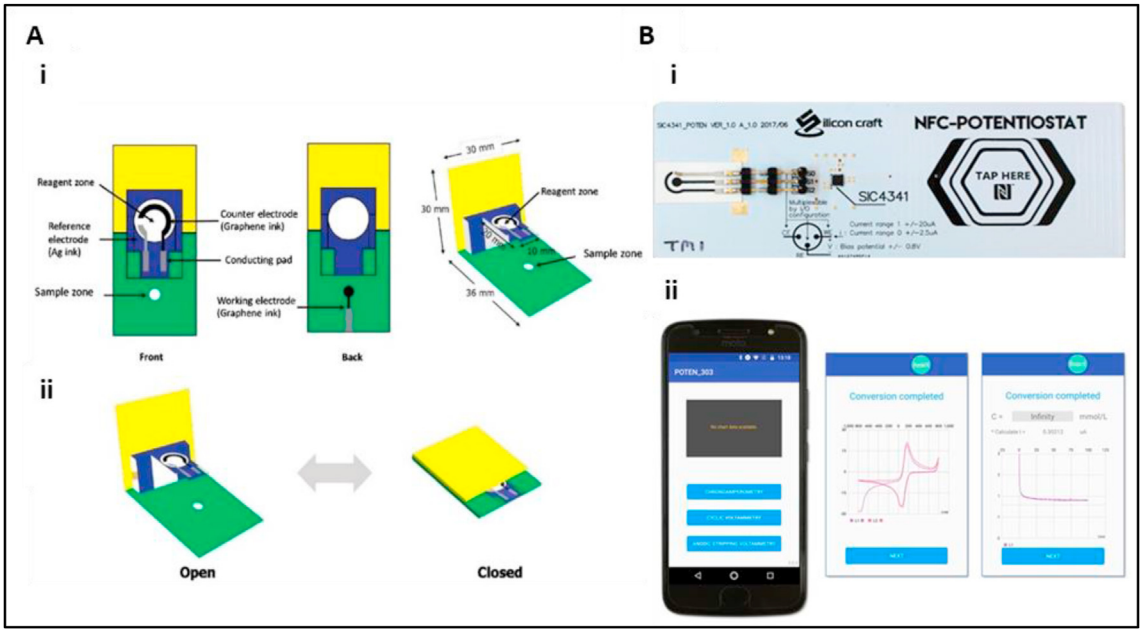

Fig. 1. (A) (i) Compartment of a pop-up PAD DNA sensor. (ii) Schematic of the pop-up PAD DNA sensor in the "open" and "closed" formats. Reproduced with permission from Ref. [77]. (B) (i) The image of portable NFC-Potentiostat. (ii) Photographs of example data for cyclic voltammetry and amperometry, respectively. Reproduced with permission from Ref. [96].

from analytes in fluorescence detection is read using a microscope, camera, laser, or charged-coupled device. On the other hand, colorimetric methods have an advantage that the signal can be read by the naked eye without the necessity of bulky instruments [82]. In recent years, alternative readout formats such as distance, text, and time have been used with PADs [83]. They have some advantages over colorimetric-based readouts due to easier analysis of quantitative results by the end-user [84].

Electrochemical methods can provide more sensitive results compared to optical methods. The detection of target molecules occurs due to specific interactions between bio-recognition elements and target analytes via covalent or non-covalent bonds, and acquisition of digital signals from a transducer into a digital detector [85]. Biorecognition elements can be antibodies, aptamer and peptide for viral detection. A variety of electrochemical methods including cyclic voltammetry (CV), linear-sweep voltammetry (LSV), differential-pulse voltammetry (DPV), square wave voltammetry (SWV), electrochemical impedance spectroscopy (EIS), conductometry, potentiometry and amperometry have been used for virus sensing [86,87]. Whereas DPV and LSV are both able to measure small potential and current differences, amperometry can detect the changes in current in response to a redox reaction during biological interaction. The change in electrical resistance based on the change in the ionic strength of a solution is measured by conductometry whereas potential difference between the working and reference electrodes is measured by potentiometry due to the changes in ion activity generated via biochemical interactions.

Smartphone-based technology as a processor and detector has become attractive for viral sensing due to its portability, wireless telecommunication, rapid acquisition of results, allowing data transfer and POC diagnosis [88]. Small optical elements such as lenses, apertures, prisms, optical fibers, waveguides, and mirrors, which offer magnification, filtering, and image improvement, are used for optical systems [89]. Smartphone-based optical sensing devices use image processing sensors for capturing images of results and, subsequently, images are processed [90]. However, the variations between cameras among various mobile phone models can cause variations in results [91]. The issues with image resolution can be overcome using deep learning (DL) methods [92]. In addition to capturing images and data acquisition, smartphones can share and store the data with the use of wireless connections via cloud servers in a secure and automated fashion. In addition to optical sensing, smartphones can couple to portable potentiostats via near field communication (NFC) technology for electrochemical detection of viruses (Fig. 1B) [93]. NFC is able to transfer electrical power (~10 mW) to electronics and sensors without the need of batteries. Polyethylene terephthalate (PET) or paper is used to produce NFC tags at low-cost (~US $0.03). Internet of Things (IoT) and 5G applications will be accelerated due to NFC-based wireless power along with data transmission from inexpensive electronics and sensors. Recent advancements in smartphone-based detection and NFC technology are extensively discussed in Refs. [90,93–95].

4. Recent applications of paper-based analytical devices for virus detection

The sensitivity of PADs requires efficient immobilization of biomolecule probes such as aptamers, antibodies, ssDNA, and antigens on the electrode surface. The modification process is achieved by physical adsorption, covalent attachment, or entrapment, and should be simple, effective, and avoid impacting the recognition elements [97]. In terms of the classification, PADs have been presented into three groups, antibody/antigen-based, nucleic acid-based, and other affinity-based PADs based on type of biorecognition element and classified according to their detection methods.

4.1. Antibody/antigen-based PADs for viral detection

Antigens or antibodies can used as biorecognition elements for the development of immunosensors for viral detection. Whereas antigens bind to the host cell receptor, antibodies are glycoproteins produced after a few days and are specific to virus antigens [98]. Antibodies are also widely used as the recognition element in virus sensors. For virus detection, monoclonal antibodies (mAb), polyclonal antibodies (pAb) and antibody single-chain variable fragments (scFv) have been used [99]. mAbs are more specific than pAb because mAbs bind to a single epitope while pAbs bind to different epitopes on a single antigen [100]. However, mAbs are more expensive than pAbs due to their longer time for production [101]. On the other hand, scFv fragments are smaller and have less variability compared to intact antibodies but require additional processing steps to be used [102].

Both label-free and labeled (sandwich) immunoassay formats are used with PADs. While label-free PADs can directly detect virus particles, label-based methods rely on sandwiching antigen between capture and detection antibodies with a label such as an enzyme, a nanomaterial, or biotin. mAbs are mostly used as the capture antibody whereas pAb is frequently used as the detection antibody. Electrostatic, hydrophobic, and van der Waals interactions, and covalent bonding strategies have been used for immobilization of antibodies. Although non-covalent strategies are simple to perform, they result in reduced antigen-binding capacity, stability and reproducibility due to random orientation of antibodies on the electrode [103]. Covalent immobilization of antibodies is employed due to reaction between modified electrode surfaces and amine, carboxyl, or thiol functional groups of the antibodies using cross-linkers such as glutaraldehyde, 1-ethyl-3-(3-dimethylaminopropyl)carbodiimide (EDC), and N-hydroxysuccinimide (NHS). While glutaraldehyde is used to activate amino groups on surface to attach antibodies via imine bonds [104], EDC/NHS coupling is used to activate either amine or carboxyl-functionalized electrode surface for more stable immobilization of antibodies via amide bonds [105]. Immobilization strategies of antibodies are reviewed in detailed in Refs. [106–109]. Blocking reagents such as bovine serum albumin (BSA) are used to block non-specific hydrophobic binding sites on the surface [110].

4.1.1. Optical detection

Although lateral flow immunoassays (LFIAs) are rapid, they usually lack quantitative results. Fluorescence-based LFIAs provide quantitative or semi-quantitative detection, however, traditional fluorescent dyes have low stability which is not ideal [111]. In addition, fluorescence-based LFIAs require a dedicated reader. The issue of dye stability can be overcome by using lanthanide-doped polystyrene nanoparticles (LNPs) [112]. Chen et al. developed an LFA based on LNPs for detection of *anti*-SARS-CoV-2 IgG [113]. A nitrocellulose membrane was treated with recombinant nucleocapsid phosphoprotein of SARS-CoV-2 and goat anti-rabbit IgG. Mouse anti-human IgG antibody labeled with synthesized LNPs via EDC/NHS cross-linker was used as a fluorescent agent. Diluted serum samples were tested in 10 min. Another LFA based on a signal-amplifiable mesoporous silica nanoparticles (MSNs) was developed to detect avian influenza viruses (AIV) and other viral avian-origin diseases by Jung et al. (Fig. 2A) [114]. Although conventional MSNs have been utilized owing to their properties such as porosity, high stability and biocompatibility, they have small pores (~3 nm) which led to obtaining blocked surface during immobilization process due to the large size of biomolecules. In this

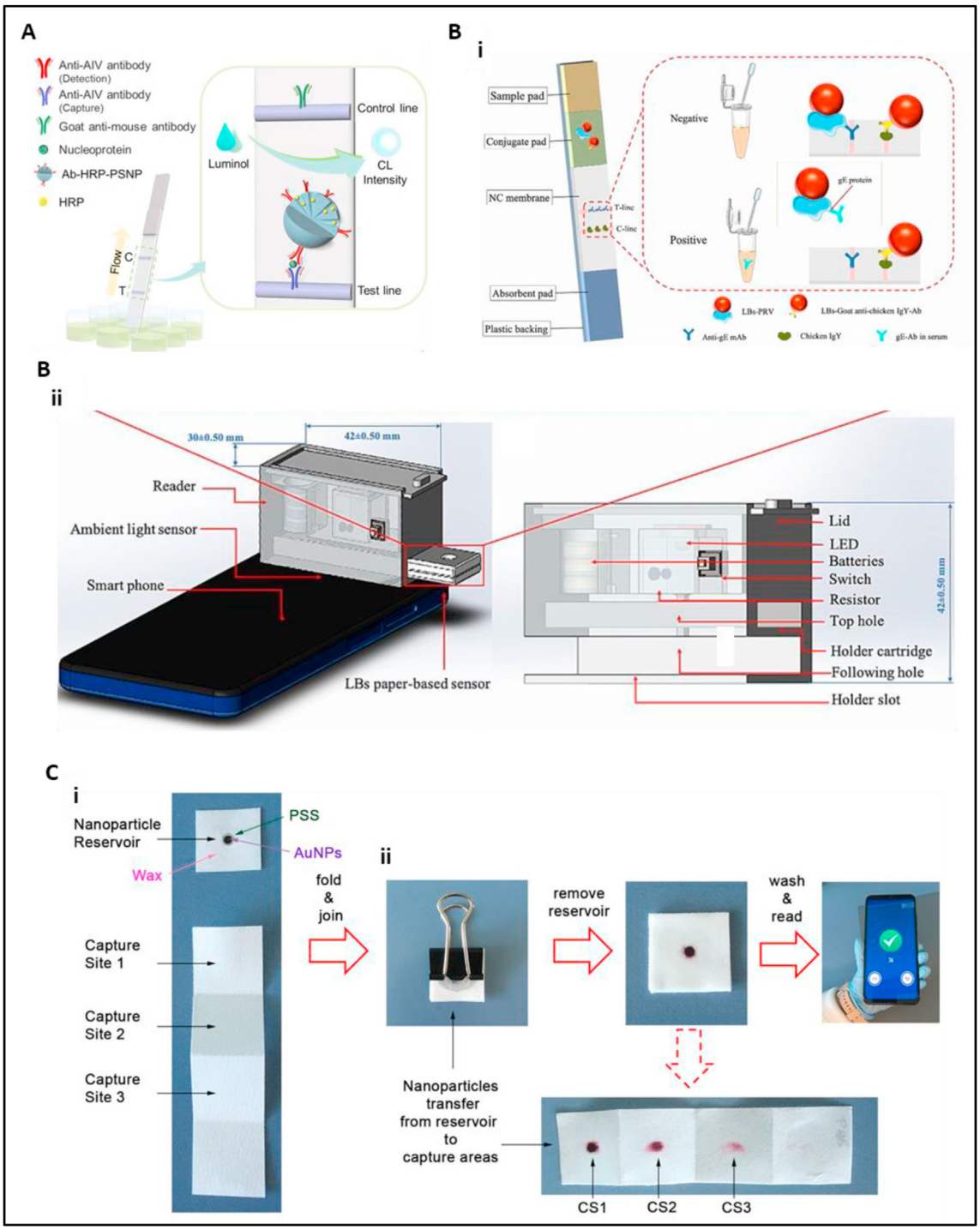

Fig. 2. (A) Schematic illustration of porous silica nanoparticle-based chemiluminescent lateral flow immunoassay (CL-LFA) platform for the detection of avian influenza virus (AIV) nucleoproteins. Reproduced with permission from Ref. [114] (B) (i) LFA for PRV gE-Ab detection. (ii) A smartphone with an ambient light sensor. Reproduced with permission from Ref. [115]. (C) (i) Photographs of the PAD and (ii) key analytical steps for detecting IL-6. Reproduced with permission from Ref. [118].

study, the issue was overcome by generating MSNs with controlled pore sizes to effectively bind biomolecules of different sizes including antibody, HRP, and BSA. After thiol-terminal modified porous silica nanoparticles were prepared, *anti*-AIV Ab was immobilized on NPs via sulfo-SMCC as a cross-linker. Then, maleimide-modified HRP was prepared using sulfo-SMCC and, conjugated to the Ab-PSNPs solution followed by blocking with BSA. Since random immobilization of HRP occurred due to the addition of HRP first and decreased the ability of antibody attachment on the MSNs, the antibodies were first immobilized to the external thiol groups of MSNs followed by HRP attachment to the remaining thiol groups between the pores. *Anti*-AIV capture Ab and goat anti-mouse immunoglobulin (IgG) were dispersed on NC membrane LFA strip. In the meantime, AIV samples were incubated with the Ab-HRP-PSNPs nanoprobe in the well plates for 15 min. Finally, LFA test strips were dipped into the wells and luminol

solution was added to the signal zone. Generated chemiluminescence signals were analyzed using a smartphone and 'Image J' software. This conjugation strategy enables large amount of antibody loading for improved binding to the target antigen and signal intensity. The optimized LFA was used to detect LPAI H9N2, H1N1, and HPAI H5N9 viruses and LODs were found as $10^{3.5}$ EID_{50}/mL, $10^{2.5}$ EID_{50}/mL, and 10^{4} EID/mL, respectively, which is 20–100 times lower than that of a commercial AIV rapid test kit. The LFA was used to test 37 clinical samples with high sensitivity and specificity.

Although LFA readers have been used directly with smartphone cameras to capture images and digitally process test results using software, the variation in pixilation and focal lengths between various smartphone cameras limits accuracy. To address this issue, Xiao et al. developed a LFA reader based on the ambient light sensor of a smartphone device, which is more sensitive and consistent compared to conventional readers, for detection of porcine epidemic diarrhea virus (PEDV) [40]. The device was composed of a switch, a resistor, three batteries and a 520 nm LED, which were integrated into a 3D-printed holder with two light transparent holes. While the top hole was attached to the lateral flow immunoassay (LFIS)'s light transparent hole, the other hole was attached to the ambient light sensor. The 3D-printed also includes a holder slot which can be easily adapted to any smartphone. After AuNPs-colored bands occurred on the NC membrane, the analyte concentration was analyzed with the LFIS reader. The operation of the reader is based on projecting emission of the light by the LED over the NC membrane. Then, the ambient light sensor of the smartphone was used to acquire the light intensity signals and free android app Light Meter was used to display. A commercial PEDV-LFIS was successfully used as a proof-of-concept and LOD was found as s 0.055 μg mL^{-1} in spiked swine fecal samples using the Light Meter app for transmission of light intensities. It takes 2 h to fabricate the reader with total cost of $1.30. The reader has advantages of being low-cost and compact without the necessity of a large dark field. The same group further improved the sensing system for diagnosing wild-type PRV infection versus vaccine immunization in swine (Fig. 2B) [115]. Here, PRV-gE antibodies were used as an indicator of PRV presence since they distinguish individual serum infected by wild-type PRV from vaccine immunization. At first, PRV was labeled with latex beads (LBs). Whereas a mixture of LBs-PRV and LBs-goat anti-chicken IgY mixture was dispersed onto the conjugation pad, PRV-gE Ab and chicken IgY were used coat the T-line and C-line, respectively. Once the serum is introduced to the sample pad, the PRV-gE Ab first binds to the LBs-PRV followed by migration to the adsorbent pad. Positive sample results in combination of the LBs-goat anti-chicken IgY and the chicken IgY on the C-line whereas the LBs-PRV do not bind the PRV-gE Ab on the T-line. Once the reaction was completed, light intensity from the T-line were analyzed with the smartphone reader due to the use of ambient light sensor. Swine clinical samples were tested in 15 min and found good agreement (98%) between commercial gE-ELISA kit.

In addition to fluorescence and chemiluminescence detection methods, colorimetric method has been used to detect viruses. Due to COVID-19 pandemic, simple and portable sensing devices are highly desirable for screening the disease. Recently, it has been suggested that serum IL-6 levels are a prognosis biomarker for COVID-19, which is between 5.1 and 18.8 pg mL^{-1} for mild cases and 22.5–198 pg mL^{-1} for moderate/severe cases [116,117]. Adrover-Jaume et al. developed a paper-based colorimetric immunosensor for detection of IL-6 in blood and respiratory samples from COVID-19 patients (Fig. 2C) [118]. A reservoir was created by using paraffin to define hydrophobic barrier on a square piece of paper and filled with polystyrene sulfonate (PSS). Then, AuNP-conjugated antibodies were introduced to the reservoir. The origami configuration was generated by folding a filter paper in 3 layers and samples were added to three capture zones. Finally, antibody loaded paper was combined with 3D origami paper to transfer NPs to the detection zones. The sum of three signals formed at each capture zone was analyzed with a smartphone app using densitometry. The device enables rapid screening of COVID-19 (less than 10 min) at PON with LOD of 10^{-3} pg mL^{-1}.

4.1.2. Electrochemical detection

Electrodes can be also modified with nanomaterials to enhance conductivity of electrochemical PADs (ePADs). Nanomaterials have been employed to modify electrode surface to detect viruses owing to their biocompatibility and high sensitivity [119]. Nanomaterials have a significant impact on efficient immobilization of bio-recognition elements on PADs. Nanoparticle-modified electrodes are extensively presented in Ref. [120]. Carbon-based nanomaterials including carbon dots (CDs), carbon nanotubes (CNTs), and graphene are rich of carbon element and classified as zero- (0D), one- (1D), and two- (2D) dimensional carbon nanomaterials [121]. The 2D carbon allotrope graphene can be covalently functionalized to obtain graphene oxygen derivatives such as graphene oxide (GO) and reduced graphene oxide (rGO) [122]. GO and rGO have been widely used to modify electrochemical devices via drop-casting, spin coating, and ink-jet printing due to their low cytotoxicity, hydrophilicity, and reactive functional groups [123]. In this context, Yakoh et al. developed an electrochemical PAD (ePAD) for detection of SARS-CoV-2 antibodies (Fig. 3A) [124]. The 3D origami device consists of three folding layers including a working ePAD, a counter ePAD and a closing ePAD. While the electrodes were screen-printed, the hydrophilic center of each zone was created by a wax barrier to allow the solution flow through to the test area. The graphene oxide (GO) solution was prepared and drop-casted on working ePAD and, the spike protein receptor-binding domain (SP RBD) of SARS-CoV-2 was immobilized via EDC/NHS. SARS-CoV-2 antibodies IgM and IgG were individually detected by SWV and the LODs were found as 1 ng mL^{-1} in the linear range from 1 to 1000 ng mL^{-1} in 30 min. The device configuration has advantage that the closing ePAD prevent the biohazard sample being exposed to the environment after analysis. The obtained LOD using ePAD was found to be three orders of magnitude more sensitive than colorimetric LFAs. However, LOD of the device was not sufficient to test SARS-CoV-2 in real nasal swab specimens. Another carbon-based nanomaterial was used to develop an electrochemical immunosensor for detection of SARS-CoV-2 by Eissa and Zourobto [125]. At first, screen-printed electrodes were modified with carbon nanofibers (CNF) via drop-casting. Next, diazonium salt was produced and used to functionalize CNF-modified electrode by electrografting. Finally, SARS CoV-2 nucleocapsid (N) protein was immobilized on the carboxyphenyl-modified-CNF electrodes using EDC/NHS coupling. A piece of cotton fiber was used to fabricate the cotton-tipped immunosensor for rapid and low-cost virus detection by combining sample collection and detection in a single platform without the need of sample preparation. A competitive assay was used to detect virus antigen in the presence of a fixed amount of N-protein antibody in the sample solution. The higher the concentration of free antigen causes the smaller amount of antibody available to attach to the antigen on the electrode surface, which was detected using SWV. The interaction between the antibody and antigen on the immunosensor resulted in an increase in the reduction peak current of the ferro/ferricyanide redox solution since the positively charged antibodies attracted to the redox anions, leading to improved signal. The immunosensor had an LOD of 0.8 pg mL^{-1} for the N antigen with a linear range 1–1000 ng mL^{-1}, showing no cross-reactivity with antigens from

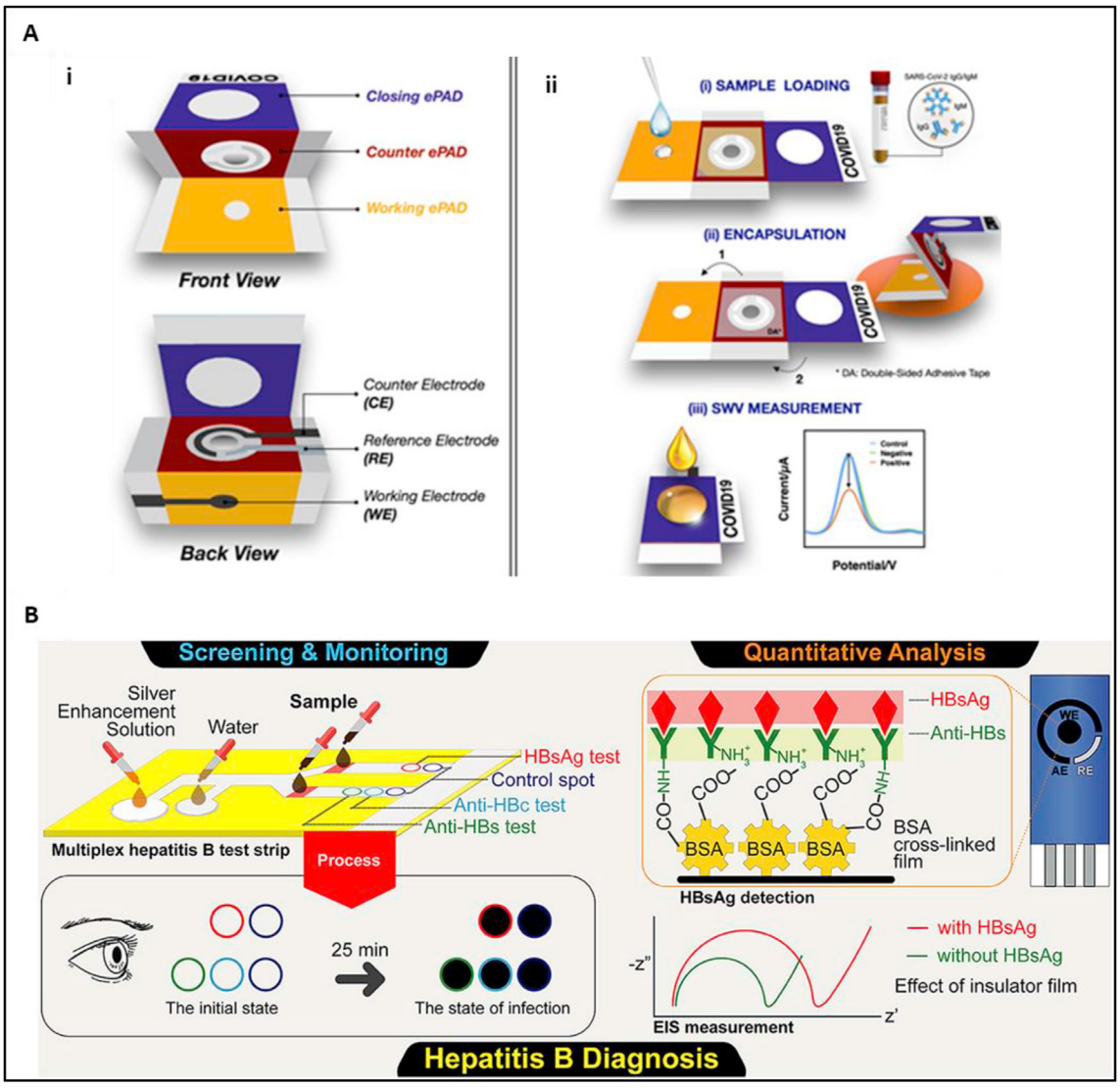

Fig. 3. (A) Schematic illustration of the (i) device components and (ii) detection procedure of the COVID-19 ePAD. Reproduced with permission from Ref. [124]. (B) (i) The developed multiplex hepatitis B test strip, and (ii) the processing steps of electrode modification. Reproduced with permission from Ref. [132].

influenza A and HCoV, The PAD could be connected to a portable potentiostat to acquire signal read-out via smartphone for POC diagnosis of COVID-19.

In addition to carbon-based nanomaterials, other nanomaterials have been used for developing electrochemical ePADs to detect viruses due to their advantages such as portability, low-cost and high sensitivity [126]. Magnetic nanoparticles (MNPs) are used to rapidly separate targets from a complex mixture of matrix substances by facilitating mass transport to the sensing area via magnetic control. Owing to the use of MNPs along with electrochemical devices, the preconcentration of the sample is achieved, allowing decreased analysis time and increased sensitivity [127]. For example, a MNP-based immunosensor was developed by Fabiani et al. to detect SARS-CoV-2 [128]. The electrodes were fabricated via screen printing using a transparent and flexible polyester support and then modified with carbon black. Antibodies for both SARS-CoV-2 proteins, S protein and N protein, were immobilized on MNPs followed by attachment of detection antibody labeled with alkaline phosphatase enzyme to generate the antibody-antigen sandwich. Preconcentrated MNPs provide enhanced enzymatic by-products that have a close contact with electrode surface resulting in improved sensitivity. In the presence of alkaline phosphate enzyme, 1-naphthol was obtained as enzymatic by-product from 1-naphthyl phosphate as the substrate. The electrochemical measurement was performed using DPV via a commercial portable potentiostat (PALM SENS). S- and N-protein in untreated saliva were analyzed and the LODs were found as 19 ng mL^{-1} and 8 ng mL^{-1} for S- and N-protein in 30 min, respectively.

Recently, the use of smartphones along with electrochemical sensors has gained interest for POC tests. Smartphones can wirelessly transfer data to a computer for analysis and storage. A smartphone functionalized with advanced computing functions and data transmission could be adapted to sensing platforms for obtaining POC devices to enhance clinical decision making and decrease treatment delays [129]. Near Field Communication (NFC) is a wireless technology that enables communication between smartphones and electronic tags [130]. NFC sensors provide to acquire data without physical connections; thus, it is possible to perform real-time monitoring of analytes. Recently, Teengam et al. presented a NFC-enabling smartphone-based immunosensor to detect hepatitis B virus [96]. The device includes an NFC antenna, a potentiostat circuit made in silicon, and connections to an

electrode, which is operated with an app. After screen-printed graphene electrodes (SPGE) were functionalized with gold nanoparticles (AuNPs), β-cyclodextrin (β-CD) were used to modify the electrode surface via electropolymerization and for immobilization of antibodies. The modification steps were verified by EIS and CV. The label-free immunosensor showed linear response between 10 and 200 μg mL^{-1} with a LOD of 0.17 μg mL^{-1} Hepatitis B surface antigen (HbsAg) in the presence of $(Fe(CN)_6)^{3-/4-}$ redox couple using amperometric detection. The developed NFC potentiostat-based sensing platform overcome the POC challenges due to its rapid response. In addition, it is low-cost (less than $10 each) and easily be adapted for detection of COVID-19. Another HbsAg electrochemical immunosensor with lower LOD than previously mentioned report was developed by Rezki et al. [131]. Here, an amine-functionalized metal-organic framework (MOF) nanospheres were synthesized via solvothermal method. MOF nanomaterials provide sensitive detection since they have open micro- and mesopores for enhanced functionalization and produce electrochemical signal due to its electroactive characteristics. The antibodies were covalently linked to aminated Cu-MOF nanospheres via EDC/NHS coupling. CV, EIS and DPV were used to perform electrochemical measurements and linear range was found as 1 ng mL^{-1} -500 ng mL^{-1} with a LOD of 730 pg mL^{-1} HBsAg. In another study, Akkapinyo et al. developed a multiplex immunochromatographic strip test and electrochemical immunosensor for screening hepatitis B virus (Fig. 3B) [132]. Three hepatitis B serological markers including HBsAg, hepatitis B surface antibody (*Anti*-HBs) and hepatitis B core antibody (*Anti*-HBc) are used for clinical diagnosis of hepatitis B [133]. While HBsAg is the indicator of positive hepatitis B infection, the presence of *anti*-HBs shows the recovery from the infection. *Anti*-HBc, which is an antibody the hepatitis B core protein, exist either in the phase of infection or recovery from HBV [134]. The strip developed test strip consists of four zones for three essential hepatitis B markers and the negative control. In addition to conventional pads used in LFAs, an enhancement pad made from chromatography paper was included in test strip in this study. Patterning of the enhancement pad included a silver enhancement pad and a washing pad was wax printed on the chromatography paper. The conjugate pads were saturated AuNPs conjugated *anti*-HBs antibodies and rabbit anti-mouse antibodies as signal generators on the test strip. Three proteins including hepatitis B surface antigen (HBsAg), hepatitis B core antibody (HBcAg) and mouse anti-rabbit antibodies were immobilized on NC membrane to form test and control spots for antibody detection. HBsAg in the sample was detected by AuNPs-Anti-HBs at the conjugate pad followed by capturing with *Anti*-HBs antibodies on the NC membrane. As a result of the immobilization, a red signal was observed at the T-line whereas the signal occurred in C-line due to the complexation of AuNPs-Anti-HBs and goat anti-mouse antibodies. Here, silver enhancement solution was used to enhance the signal intensity by increasing the NPs's size due to the deposition of silver on AuNPs's surface. The same concept was used for the *Anti*-HBs and *Anti*-HBc tests in corresponding spots of the device. For quantitative detection, a SPE was modified with BSA-film to immobilize the hepatitis B surface antibodies via EDC/NHS coupling for detection of HBsAg. The test strip had LODs of 0.5, 0.3 and 0.1 μg mL^{-1} for HBsAg, *Anti*-HBs and *Anti*-HBc, respectively, whereas the electrochemical SPE showed a LOD of 2.1 ng mL^{-1} HBsAg within a linear range 5−3000 ng mL^{-1} using EIS. To obtain the electrical response during EIS measurements, a small amplitude AC signal is periodically applied. Real and imaginary impedance components are plotted to obtain Nyquist plot, which indicates the impedance within frequency range. The straight diagonal line of a Nyquist plot at lower frequencies shows a diffusion-controlled redox process whereas the semicircle of a Nyquist plot shows at higher frequencies shows charge transfer resistance (Rct) from the electrode surface to the redox couple solution. Among electrochemical methods, EIS is commonly utilized due to its ability to reveal interaction between different layers of PAD during surface modification of the electrode [135]. Since EIS is highly sensitive, it is frequently used for label-free immunosensors [136]. Principles of these electrochemical detection techniques have been broadly reviewed [49,137].

LFA strips have the advantage of enables simultaneous analysis of multiple biomarkers, allowing POC diagnosis in developing countries at low-cost. The electrochemical detection approach can be used for label-free detection of HBV with cost-effective and easily mass producible way. In a recent study, a label-free electrochemical immunosensor based on bimetallic Au@Pt nanoparticles, Prussian blue (PB), and reduced graphene oxide-tetraethylene pentamine nanocomposite (rGO-TEPA) for detection of HBsAg was presented by Wei and coworkers [138]. rGO/PB-Au@PtNPs composite was produced by mixing Au@PtNPs with rGO-TEPA/PB nanocomposites prepared via in-situ reduction. Here, rGO-TEPA was used to enhance electrocatalytic function of PB NPs and adsorption of noble metal (Au@Pt) NPs owing to their abundant amino groups on the surface. After the screen-printed electrode was modified with the nanocomposite, hepatitis B antibody (HBsAb) was immobilized on the electrode surface. Au@PtNPs provide efficient antibody attachment and analyte contact with active sites on the working electrode surface due to their large surface area. The immunosensor exhibited a linear range from 0.25 pg mL^{-1} to 400 ng mL^{-1} with a LOD of 0.08 pg mL^{-1} using DPV.

Although a variety of immunosensors have been proposed, there are still challenges. Non-specific adsorption may occur because of poor quality of antibodies immobilized on electrode surface and lack of control of electrode surface chemistry [139]. Engineered recombinant antibodies offer modifications with tags or labels and antibody fragments, which attach to single antigen epitopes. On the other hand, antibodies can be affected by pH, salt concentration and/or temperature changes [140]. In addition, antibodies used for whole virus particles can target epitopes that change due to changes in the viral genome [141]. Recently, antibodies against the SARS-CoV-2 S protein of the viral envelope have been used in construction of immunosensors against SARS-CoV-2 [142]. There are commercial antibodies against the S, E, M and N proteins of SARS-CoV-2, however, their specificity has not been presented so far. Thus, antibodies should be screened carefully during virus immunosensor development.

4.2. Nucleic acid-based PADs for viral detection

Unlike immunoassay-based methods, nucleic acid amplification-based methods are not based on detection of antibody or antigens produced by host cells. Viral pathogens include genomes, which encode them, can be used as a marker of the infectious diseases due to their specific genetic information. To detect target nucleic acids, target-specific primers are designed based on complementary base pairing. DNA/RNA probes are used as recognition elements to construct nucleic acid-based devices due to specific hybridization reactions between DNA-DNA or DNA-RNA [143]. However, extraction of the DNA/RNA sequences in a viral pathogen is not straight forward and should be performed efficiently. High temperature, chemical reagents and mechanical force are used for virus lysis to obtain the nucleic acid [144]. Nucleic acid amplification methods including thermal cycling amplification, isothermal amplification, and rolling circle amplification are used to improve the concentration of viral nucleic acid for detection [145]. Thermal cycling has drawbacks because temperature control is necessary with the use of complex heating elements, limiting POC applications. Isothermal

techniques have been developed to overcome this problem by eliminating thermocycling steps. Nucleic acid amplification approaches for biosensing are discussed in Refs. [146,147].

4.2.1. Optical detection

In fluorescence detection of viruses, nucleic acids are modified with fluorescein derivatives such as ethidium bromide dye, SYBR green or TaqMan probe, which emit fluorescence under LED light sources [146]. Recently, entropy-driven amplification strategy as a novel isothermal nucleic acid amplification method has been presented for highly sensitive detection of nucleic acids. In a recent study, an entropy-driven amplification strategy-assisted LFA was developed for detection of influenza virus H1N1-RNA [148]. At first, the fluorescent nanospheres (FNs)-DNA conjugates were prepared. Then, entropy-driven reaction sample was obtained using the biotin labeled substrate (S) which is a three stranded hybridization complex (R/L/by-product, P strands). Whereas the reporter DNA (strand R) was labeled with a FN, the linker strand (L) was modified with biotin to attach streptavidin. Streptavidin-biotinylated capture DNA and streptavidin were dispensed on the NC membrane to generate T-lines and C-lines, respectively. The cascade strand displacement reaction occurred in the presence of target, producing strand R. After the hybridization reaction, amplified fluorescence of the nanosphere was captured using a UV lamp and a digital camera. The device LOD was 2.02 pM influenza virus H1N1 RNA in human serum sample, which is 746-times larger than the non-amplified assay. The stability of the device was up to 6 months at 4°C. Due to the use of the entropy-driven amplification, the total number of base pairs remained constant, decreasing circuit leakage and obtaining high sensitivity for the target nucleic acid detection. The proposed sensing strategy is advantageous over traditional nuclease-based signal amplification because the system does not require enzymes. Another isothermal amplification method, loop-mediated isothermal amplification (LAMP), is used for nucleic acid amplification. Four primers including the forward inner primer and backward inner primer (FIP and BIP), and forward and backward outer primers (F3 and B3) are used to bind to six unique sequences on the target. LAMP is based on Bst polymerase which is operated at 55–65°C. LAMP shows high amplification capacity up to 109-fold, producing signal with improved specificity [149,150]. Therefore, LAMP has become a promising method particularly for paper-based systems for viral detection. Seak et al. developed a lab-on-paper for all-in-one molecular diagnostics (LAMDA) of zika, dengue, and chikungunya virus from human serum (Fig. 4A) [151]. The 3D-PAD was designed by integrating lateral and vertical flows. Sampling, extraction, amplification, and detection were combined on a single paper chip, which includes loading pad, serum loading pad, connection pad, absorbent pad, and amplification, by stacking. A polyethersulfone membrane was wax-printed and used as a fluidic channel pad. While functional parts were treated chemical solutions, the transfer pad was treated with LAMP reagents. After serum sample containing target virus RNA was introduced to the serum loading pad, target RNA molecules were obtained owing to dried lysis buffer. The loading pad was used for the washing step and transferring the target RNA to the amplification area via lateral flow. Then, purification and concentration of nucleic acids was achieved due to the presence of chitosan on the binding pad. Finally, target specific reverse transcription-LAMP amplification occurred in the reaction pad with increased pH via vertical flow, obtaining fluorescence signal by hydroxylnaphthol blue (HNB) molecule in the presence of green light source. Zika, dengue, and chikungunya virus RNA in human serum was simultaneously detected in different zones on the reaction pad due to the fluidic separation by wax printing in 1 h at 65°C. Serum containing 5400 copies of zika virus, 5700 copies of dengue virus, and 4500 copies of chikungunya virus was successfully tested. The paper chip offers a portable, mass-producible, and low-cost platform for virus detection in an automated fluidic flow. However, the platform requires a portable reader and heater is necessary for signal analysis and incubation step, respectively, which limit the devices use for POC diagnosis. This issue can be overcome by using a proper algorithm during real-time signal read-out.

Colorimetric detection, which is based the color change of chemical reaction, is an alternative detection technique for nucleic acids. For example, a paper-based nuclease protection assay has been developed by Noviana et al. [152]. The sample was pretreated on-chip using chitosan-modified paper to increase selectivity due to the elimination of possible interferents from the reaction and pre-concentrate the nucleic acids. After a 5′-digoxigenin- and 3′-biotin-labeled oligonucleotide probe and the target were hybridized, unhybridized probe, target, and single-stranded non-target DNA were cleaved by digestion of P1 nuclease (from *Penicillium citrinum*). Nitrocellulose membrane, which was modified with an *anti*-digoxigenin antibody, was utilized to capture the labeled probe-target hybrids. Since streptavidin-conjugated horseradish peroxidase (Strep-HRP) and, tetramethylbenzidine (TMB) and hydrogen peroxide as an enzyme-substrate pair were applied on the membrane, a blue line was observed as colorimetric signal due to the presence of the target DNA. The colorimetric signal can be quantified using a cellphone camera and image analysis software. It is possible to detect sub-femtomole of target DNA with high specificity via the proposed assay within 2–3 h. The advantage of the paper-based detection platform is that the detection limit was improved by ~5-fold due to sample pretreatment chitosan-modified paper on-chip. Although, the sensor had higher LOD compared to the amplification-based techniques, the developed colorimetric sensing system is promising for POC screening of COVID-19 especially in resource-limited areas. Moreover, chemical coloration and enzyme cleavage substrate coloration techniques have become popular due to the advancements in nucleic acid detection technology. For example, Sun et al. developed a colorimetric PAD based on a simple and low-cost colorimetric assay based on a cell-free system and toehold-switch technique for detection of GII.4 and GII.17 genotypes of norovirus (Fig. 4B) [153]. Toehold-switch sensor is an RNA-based translational regulator, which is able to regulate protein synthesis including the enzyme β-galactosidase (LacZ). The switch RNA includes a hairpin module with a start codon. While its 5′ end consists of a complementary sequence to the target sequence, its 3' end consists of the coding sequence of the regulated gene. The codon is activated to initiate the translation of the lacZ gene after the target sequence is encountered by the switch RNA. The detection is based on cleavage of a yellow color substrate namely Chlorophenol red-β-D-galactopyranoside (CPRG) via LacZ protein, producing a purple product. The paper was first pretreated with BSA. Then, the paper was cut into paper disks followed by treating with the cell-free reaction mixture and placed in 96-wells plate. To obtain cell-free system, the paper disks were dried in a lyophilizer. Plasmid DNA containing the target sequence was dropped onto the paper and a color change was observed with naked eye. The assay generated an LOD of 0.5 pM and 2.6 fM for the GII.4 and GII.17 genotype, respectively. Herein, the stability of the lyophilized system was investigated using trehalose and polyvinyl alcohol (PVA) as protein stabilizers. While trehalose was more effective than PVA at 4°C, PVA was more stable than trehalose at −20°C. Thus, the appropriate protein stabilizer can be selected according to transportation conditions. Although the cost of the developed assay is around $20 per reaction, the costs can be reduced under $6 per reaction using self-made nucleic acid sequence-based amplification reagents instead of using commercial reagent kits. This method should be further

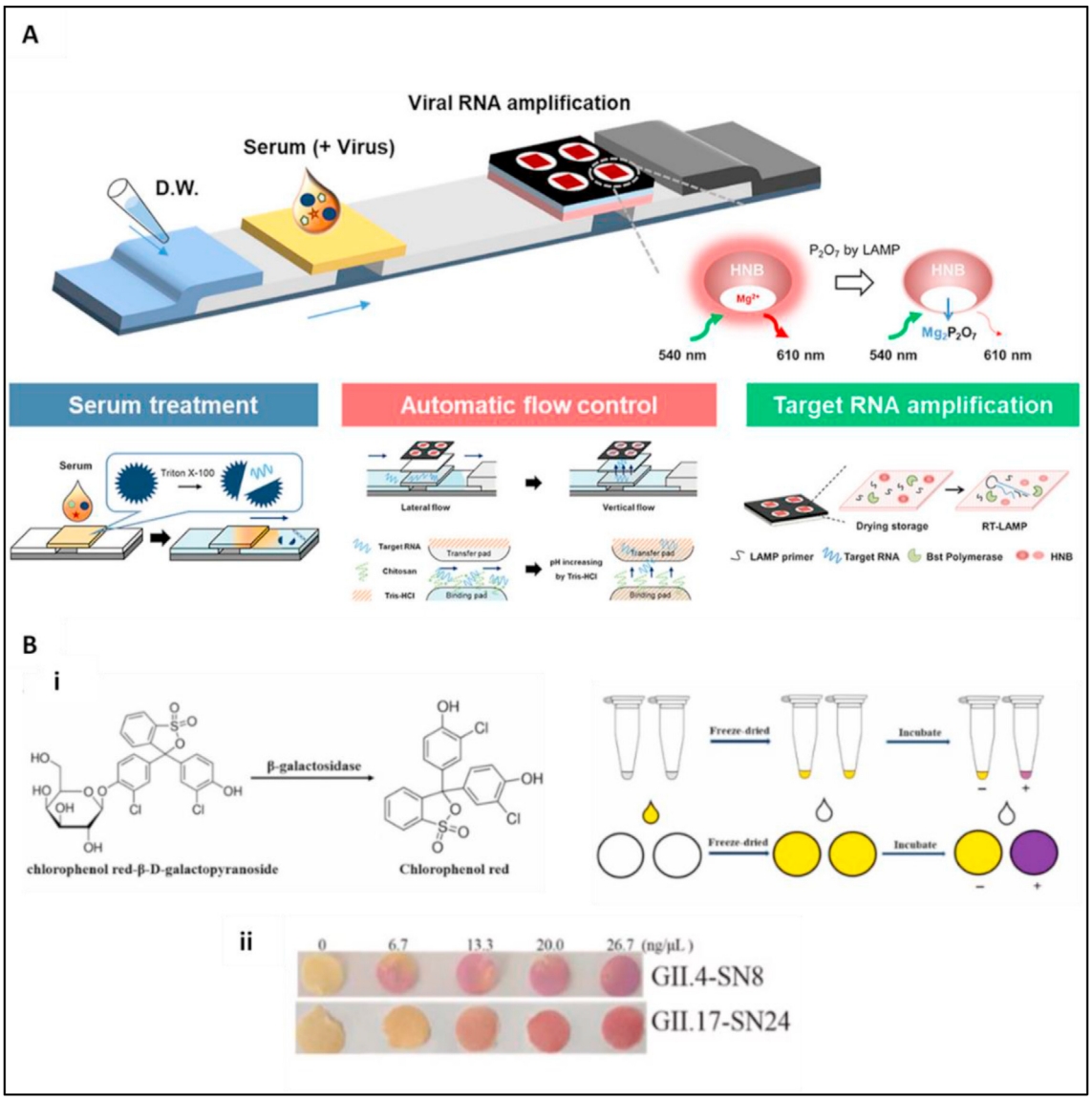

Fig. 4. (A) The lab-on-paper for all-in-one molecular diagnostics (LAMDA). Reproduced with permission from Ref. [151]. (B) (i) The mechanism of paper-based colorimetric method, and (ii) images of paper-based reactions toehold switch SN8 for GII.4 and SN24 for GII.17 detection. Reproduced with permission from Ref. [153].

developed for POC diagnosis especially in hot climate since the enzymes should be kept at low temperature. Similarly, the same group presented another colorimetric toehold switch sensor in a paper-based cell-free system for detection of respiratory syncytial virus subgroups A (RSVA) and B (RSVB) [154]. The same concept was used for construction of the PADs, and the expressed LacZ hydrolyzed chromogenic substrates due to the presence of target trigger RNA. The colorimetric signal was analyzed by a microplate reader and the LODs for RSVB and RSVA were obtained as 91 aM and 5.2 fM, respectively. The specificity of the PAD was evaluated with human coronavirus HKU1 (HCoV-HKU1) and SARS-CoV-2. The assay has an advantage that it can distinguish RSVA and RSVB without the need of sophisticated equipment.

Advancements in magnetic nano/micro beads structures has driven their use for enrichment of the target DNA from complex matrixes. To enhance sensitivity of nucleic acids, isothermal strand-displacement amplification (SDA) can be used. Two target-specific primers, a polymerase enzyme and a nicking exonuclease enzyme are necessary for amplification, which can cleave the synthesized strand between the primer and target sequence. SDA can be operated at 21–65°C, depending on the polymerase selected [155]. With the use of magnetic beads and nicking enzyme-assisted SDA, Zhao et al. demonstrated a LFA to detect hemorrhagic fever viruses including hantavirus (HTNV), chikungunya (CHIKV), dengue (DENV), and Ebola (EBOV) [156]. After biotin was used to modify the capture probe for magnetic bead separation of RNA, reverse transcription of total RNA was performed. The SDA reaction was carried out by adding the primer sequence and the nicking enzyme, Nb.BbvCI, to the reverse transcription products of each virus. The incubation process was performed at 37°C for 1 h. As a result of the amplification reaction, the products were introduced to the sample pad of the LFA, which was treated with AuNPs conjugated DNA probe. Thus, SDA-amplified products modified with AuNPs were utilized as the capture probes. A sandwich link was generated at the T-line and the LOD of this assay was 10 fM in 5 min. The LFA does not require thiolated DNA extraction and purification steps and is suitable for POC diagnosis of hemorrhagic fever virus.

For nucleic acid amplification, the degradation of nucleic acids by enzymes (nucleases) is common [157]. In recent years, Clustered Regularly Interspaced Short Palindromic Repeats (CRISPR)-associated nuclease (Cas)-based sensing systems have shown promise for POC sensing. Exogenous invasive genetic sequences are processed and kept in the form of short DNA sequences by CRISPR. These sequences are transcribed and processed into small noncoding RNAs when they are integrated. After that, RNAs attach to the Cas nuclease enzyme, degrading the corresponding target disease nucleic acids [158]. DNA Endonuclease-Targeted CRISPR Trans Reporter (DETECTR) DETECTR technology is a potential method to detect infectious diseases [159]. Sensitive POC detection of nucleic acids can be employed with the use of RNA-guided target-recognition-triggered collateral cleavage as an amplifier. Cas effector proteins such as Cas9, Cas12, Cas13 and Cas14 have been used as target sequence recognition elements along with a variety of LFAs for nucleotide sensing with LODs down to zeptomolar (10^{-21} M) [160]. Broughton et al. reported a CRISPR-Cas12 based LFA using SARS-CoV-2 DETECTR platform combined with reverse transcription-LAMP (RT-LAMP) for detection of SARS-CoV-2 in clinical samples [161]. Cas12 gRNAs were designed for detection of three SARS-like coronaviruses including SARS-CoV-2, bat SARS-like coronavirus and SARS-CoV in the E gene after primers targeting the E (envelope) and N (nucleoprotein) genes of SARS-CoV-2 were designed. The DETECTR assay consists of RT-LAMP reaction for extraction of SARS-CoV-2 RNA from swabs at 62°C, generating dsDNA products, and Cas12 detection reaction of predefined coronavirus sequences at 37°C. After *trans*-cleavage assay with Cas12a, a lateral flow strip was then dipped into the reaction tube. The assay can be performed in less than 40 min. The signal produced at the T-line was read out in 2 min using a FAM-biotinylated reporter molecule, which captured labeled nucleic acids. The signal intensity was analyzed using ImageJ for quantification and the LOD of the assay was 10 copies of SARS-CoV-2 RNA per microliter of RNA extract. The method was validated using patient samples positive for COVID-19 and other viral respiratory infections. The proposed CRISPR-based DETECTR assay offers an alternative platform to the US Centers for Disease Control and Prevention SARS-CoV-2 real-time RT-PCR assay. Also, CRISPR-Cas-based systems are advantageous over PCR-based methods because specific primers are used during isothermal amplification. POC detection could be achieved by incorporating portable microfluidic-based cartridges with the assay in the future. CRISPR sensing technology is at the early stage of development, however, POC devices can be developed by coupling with paper-based lateral flow and isothermal amplification, achieving sensitive viral detection. In addition to DETECTR, specific high-sensitivity enzymatic reporter unlocking (SHERLOCK) technology is presented for paper-based CRISPR-Cas diagnostics [162]. Nucleic acid detection based on CRISPR/Cas technology is reviewed in detail in Refs. [163–165].

4.2.2. Electrochemical detection

Paper-based electrochemical biosensing platforms enable advancements in POC devices for the rapid detection of viral nucleic acids. Due to the interaction between probes and targets, the electrochemical signal generated on the electrode surface is measured in the presence of redox-active probes are $[Fe(CN)_6]^{3-/4-}$ and $[Ru(NH_3)_6]^{3+}$ complexes via electrochemical techniques [166]. Methylene blue (MB), which is a cationic dye, is used for electrochemical detection of target DNA due to the interaction between free guanine base and the cationic amino groups of MB. As a result of hybridization between ssDNA and the target DNA, the signal is decreased due to the reduced availability of free guanine [167]. Although nucleic acid-based ePADs show high specificity and stability, efficient hybridization is a challenging task to obtain desired sensitivity [168,169]. While small amounts of probe immobilized on the nucleic acid-based PAD surface can limit analyte binding, excessive probe density can decrease hybridization efficiency due to the saturation of the device surface [170].

Loading of a high amount of capture DNA has been achieved by exploiting the graphene-based nanoparticles owing to their high surface area. For example, Rana et al. developed an ePAD based on based on oxidized (Ox) graphitic carbon nitride (g-C_3N_4) for detection of norovirus-specific DNA [171]. g-C_3N_4, which is a semiconducting material, has a large surface area, is inexpensive, possesses excellent chemical stability and improves electron transfer due to its nitrogen content [172]. The electrodes were fabricated using carbon ink on cellulose paper via screen-printing. To create hydrophobic barriers, wax printing was used. Ox-g-C_3N_4 NPs were drop-caste and the capture probe DNA was immobilized by adsorption. The device had a LOD of 100 fM using MB via DPV and showed specificity over a non-complimentary DNA. Another nanomaterial-based ePAD was developed by Singhal et al. for a multiplexed detection of dengue virus (DENV) subtypes using graphene oxide-silicon dioxide (GO-SiO_2) nanocomposites (Fig. 5A) [173]. The multiplexed PAD was fabricated using the stencil printing and, included four working electrodes and a counter electrode [174]. GO-SiO_2 nanocomposite was synthesized and used to modify working electrodes. DNA probes were immobilized via adsorption onto the electrode surface. Amplification in the signal response occurred due to conductivity of the nanocomposite. The device showed linearity between 100 pM and 1.0 μM with a LOD of 100 pM target DNA of the four serotypes of the dengue virus (DENV), DENV 1, DENV 2, DENV 3, and DENV 4. The PAD can easily be adapted for mass production and early prediction of dengue hemorrhagic fever (DHF) or dengue shock syndrome (DSS). In a recent study, Zhao et al. developed an ePAD based on calixarene functionalized graphene oxide to detect RNA of SARS-CoV-2 (Fig. 5B) [175]. Au@Fe_3O_4 nanoparticles were produced and immobilized to the capture probe (CP) labeled with thiol (HT). *p*-Sulfocalix [8]arene (SCX8) functionalized graphene (SCX8-RGO) was prepared and used for enrichment of the electrochemical mediator, toluidine blue (TB), followed by modification with AuNPs to generate Au@SCX8-RGO-TB nanocomposites. The nanocomposite was incubated with labeled signal probe (LP) and auxiliary probe (AP), respectively. CP-Au@Fe_3O_4 was incubated with target viral RNA which was extracted using commercial kits. Au@SCX8-RGO-TB-LP-AP was incubated with target-HT-CP-Au@Fe_3O_4. The final composite was drop-casted on a screen-printed carbon electrode and analyzed with DPV using with a smartphone giving a linear range between 10^{-17} and 10^{-12} M target RNA. While the 5′ -and 3′ -terminals of target sequence are complementary to CP and LP, the 5′- and 3′ -regions of AP have complementary sequences with two different LP areas, respectively. Thus, high sensitivity could be achieved with the use of CP and LP, and AP based on sequence-specific detection. The real patient samples including throat swabs, urine, plasma, feces, serum, whole blood, and saliva were tested and the LOD was obtained as 200 copies mL^{-1} SARS-CoV-2 RNA. The proposed plug-and-play diagnostic system based near-POC test is promising for sensitive detection of SARS-CoV-2. Graphene-based materials for electrochemical detection of viruses is presented in Ref. [8].

Recently, a variety of MOFs have been conjugated with DNA to electrochemically detect target DNA owing to their properties such as low-cost, large surface area and controllable porosity [176]. Although MOFs provide efficient immobilization of the target probe, they usually suffer from low electrical conductivity. Therefore, the proper design and preparation of composites is necessary to obtain enhanced conductivity. Lu et al. developed a paper-based nickel metal-organic framework (Ni-MOF) composite/Au nanoparticles/carbon nanotubes/polyvinyl alcohol (Ni–Au composite/

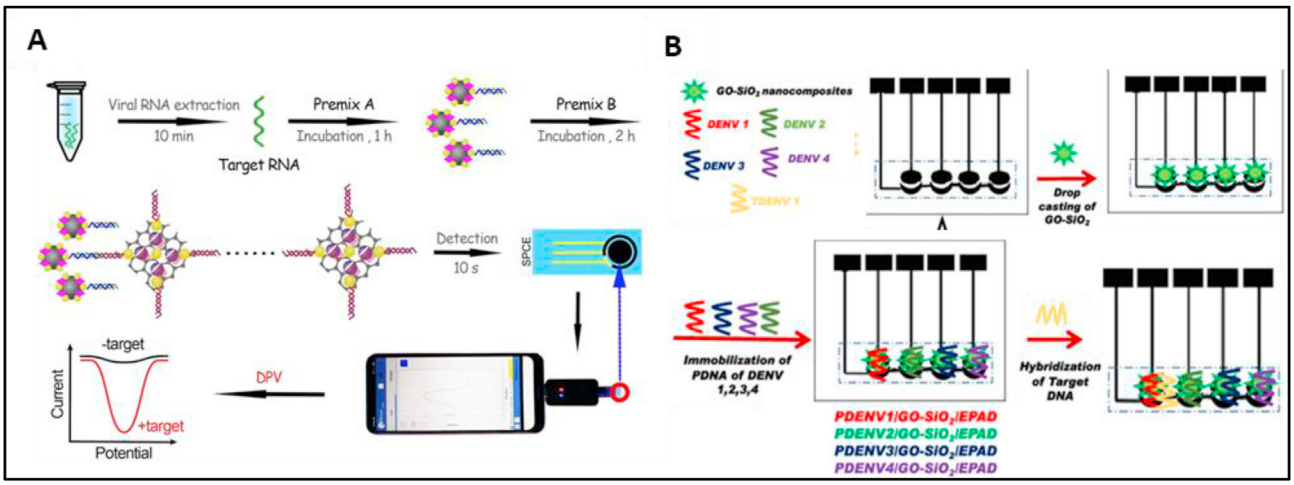

Fig. 5. (A) SARS-CoV-2 detection using the ePAD with a smartphone. Reproduced with permission from Ref. [173]. (B) Fabrication of the multiplexed PAD for specific dengue serotype detection. Reproduced with permission from Ref. [175].

CNT/PVA) film electrode for HIV DNA detection [177]. A mixture of CNT and PVA was deposited on a cellulose membrane by vacuum filtration to fabricate the working electrode. Ni-MOF composite/AuNPs was produced via one-step calcination method and drop-casted on the working electrode. Then, single-stranded DNA (ssDNA) was immobilized on the electrode surface owing to large specific surface area of MOF with hydrogen bond sources. Target HIV DNA was detected using DPV through DNA hybridization in the presence of methylene blue (MB) as a redox indicator. The current signal of MB decreased with the increase of target DNA concentration. The PAD exhibited a LOD of 0.13 nM target HIV DNA within linear range of 10 nM-1 μM. The CCP film remained after bending 200 times, showing good flexibility. The device had long stability (~20 days) and was successfully used in serum samples. Functional groups, geometry structure, size, porosity, stability of MOFs are important parameters for designing concept and the detection performance of the device. MOFs based biosensing of viruses has been extensively presented in Refs. [178,179].

4.3. Other affinity-based PADs for viral detection

In addition to nucleic acid and antibody/antigen-based PADs, other biomarkers such as glycoproteins, peptide-nucleic acids and aptamers have been used for detection of viruses. Glycoproteins contains oligosaccharide chains linked to polypeptides, which are useful for disease diagnostics [180]. Although methods such as enzyme-linked immunosorbent assay (ELISA), capillary electrophoresis, high-performance anion exchange chromatography and liquid chromatography are used for identification of glycoproteins as biological markers of pathogens, they suffer from high-cost, complicated and time-consuming pre-treatment steps, the need for skilled personnel and expensive equipment [181]. Thus, a rapid and reliable screening method is important for detection of glycoproteins, particularly for SARS-CoV-2. For example, GO and gold nanostars (AuNS) were utilized to modify screen printed electrodes by Hashemi et al. for detection of viral glycoproteins of SARS-CoV-2 [182]. Functional groups of GO were activated using 8-hydroxyquinoline (8H), EDC and NHS to attach synthesized AuNS. The active functional groups of proteins such as $-NH_2$, $-OH$, CH_3 and carbonyl functional groups were trapped on electrode surface resulting in sensitive detection of target viral glycoprotein. The detection mechanism was based on the interaction with active functional groups of viral glycoprotein, obtaining different voltage positions as a fingerprint for each virus using DPV. The LOD of 1.68×10^{-22} μg mL^{-1} with sensitivity 0.0048 μAμg.mL^{-1}.cm^{-2} toward detection of SARS-CoV-2 in clinical samples was obtained using DPV in 1 min. The device has the advantage that any extraction step prior to analysis or biomarker such antibody, DNA, antigen is not necessary to detect viruses.

Peptide nucleic acids (PNAs), which are a non-degradable DNA mimic having a neutral N-(2-aminoethyl) glycine backbone, have been used as a probe in PAD development. The specificity can be improved with the use of PNA probe owing to their strong target-binding affinity to DNA or RNA. Since there is no electrostatic repulsion between uncharged PNA backbone and nucleic acid counterpart, PNAs exhibit high affinity towards complementary DNA and RNA sequences [183]. PNAs are advantageous over nucleic acid oligomers in that they are thermally stable and resistant to degradation by nucleases and proteases [184]. In a recent study, an automated paper-based lateral flow electrochemical device (eLFA) was developed to detect by the Vilaivan and Chailapakul group (Fig. 6) [185]. A sequence of the acpcPNA (TCC TGG AAT TAG AGG) complementary with the HBV DNA target was synthesized and used as a probe due to its higher specificity and lower background currents than those of traditional probes. Wax-printing was used to pattern the nitrocellulose membrane, followed by the immobilization of acpcPNA on the detection zone. The system was assembled with other components including screen-printed electrode, sample pad and adsorbent pad using a plastic backing card. The LFA device consists of a non-delayed channel, a straight a zigzag delayed channel and a trapezoid-shaped zone for sample delivery, Au^{3+} delivery, and detection step, respectively. A gold metallization strategy was used for the signal-on electrochemical detection of the target DNA. Once the HBV DNA sample was introduced to the sample zone, the solution flowed through the non-delayed channel, hybridizing with the acpcPNA probe at the detection zone. The solution was delayed and merged with the solution flowed through the delayed channel due to the wax-printed barriers, leading to automatic and sequential application of the assay. After DNA hybridization occurred, Au^{3+} attached to the captured DNA via electrostatic interactions. Finally, Au^0-metallized DNA was generated using electrochemical reduction and the HBV DNA concentration was determined with an anodic stripping voltammetry (ASWV). A linear range between 10 pM and 2 μM HBV DNA with a LOD of 7.23 pM was obtained in 7 min with single sample loading. The developed PAD was applied to real patients' samples without the need of amplified DNA. The design of PNAs-based devices has been reviewed in Ref. [186].

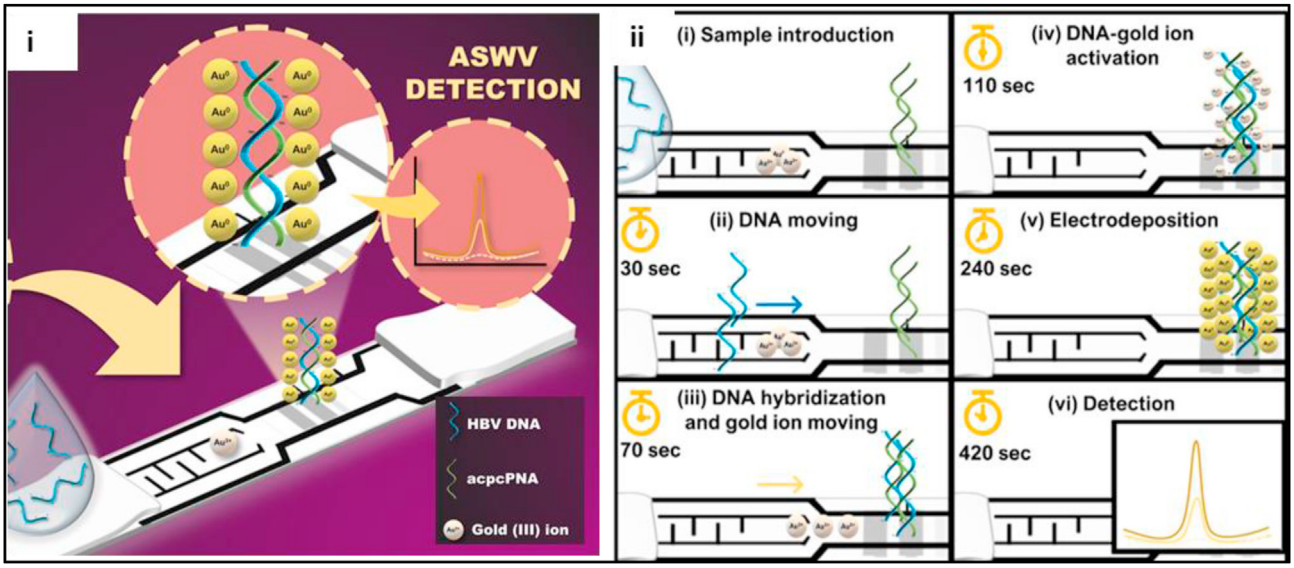

Fig. 6. (i) Schematics of the eLFA, and (ii) operation of HBV DNA detection on the automated eLFA device. Reproduced with permission from Ref. [185].

Aptamers, which are single-stranded oligonucleotides or peptides, can be used for detection of whole viral particles. They are advantageous over antibodies because they are inexpensive and easily synthesized and modified [187]. RNA aptamers are degraded by nuclease activity of RNases, which makes it difficult to develop antiviral aptamers. Since full-length membrane protein purification of viral particles is challenging, Cell-SELEX (systematic evolution of ligands by exponential enrichment), which uses whole cells instead of target proteins, has been developed to selectively bind to the target [188]. In a recent study, Liu et al. demonstrated a LFA based on magnetic enrichment and SDA to detect coat protein of red-spotted grouper nervous necrosis virus (RGNNV-CP) [189]. After AuNPs were synthesized and conjugated to DNA, AuNPs-DNA was immobilized on the conjugate pad. Streptavidin-modified magnetic beads (MBs) were coated with the C-aptamer and A-aptamer, which were incubated with RGNNV. Then, magnetic separation was

Table 1
Summary of antigen/antibody-based PADs for virus sensing.

Target	Fabrication Method	Detection Method	Label/Biorecognition element	Linear Range	LOD	Ref.
Hepatitis B virus (HBV)	screen printing	DPV	Label free/acpcPNA	0.05–100 nM	1.45 pM	[77]
HIV type 1(HIV-1) p24 antigen	wax printing	Colorimetric	*anti*-HIV-1 p24/*anti*-HIV-1 p24-HRP)	Not specified	0.03 ng mL^{-1}	[78]
anti-SARV-CoV-2 IgG	LFA	Fluorescence	lanthanide-doped polysterene nanoparticles (LNPs)	Not specified	N/A	[113]
avian influenza viruses (AIV), H9N2, H1N1, H5N9	LFA	chemiluminescent	PSNPs/antibody/HRP	Not specified	$10^{3.5}$ $10^{2.5}$ 10^{4} EID_{50}/mL	[114]
Porcine epidemic diarrhea virus (PEDV)	LFA	Fluorescence	AuNPs/LFIS	Not specified	0.055 μg mL^{-1}	[40]
Pseudorabies virus (PRV)-gE-Ab	LFA	Fluorescence	Latex beads/	Not specified	N/A	[115]
IL-6	Wax printing	Colorimetric	AuNPs-antibody	10^{-3}-10^{2} pg mL^{-1}	10^{-3} pg mL^{-1} in PBS, 1.3 pg mL^{-1} in blood	[118]
SARS-CoV-2 antibodies IgG and IgM	Wax printing and screen printing	SWV	GO/spike protein receptor-binding domain (SP RBD) of SARS-CoV-2	1–10^{3} ng mL^{-1}	1 ng mL^{-1} for each antibody	[124]
SARS-CoV-2 antigen	Screen printing	SWV	carbon nanofiber/diazonium/ nucleocapsid (N) protein/antibody	1–1000 ng mL^{-1}	0.8 pg mL^{-1}	[125]
SARS-CoV-2 S protein and N protein	Screen printing	DPV	Carbon black/-MNPs-*anti*-mouse IgG anti/SARS-CoV/Alkaline Phosphatase-labeled-Anti-Rabbit IgG Antibody	0.01–0.6 μg/mL	19 ng mL^{-1} for S protein and 8 ng mL^{-1} for N protein	[128]
Hepatitis B surface antigen (HbsAg)	Screen printing	Amperometry	AuNP/β-cyclodextrin (β-CD)/	10–200 μg/L	0.17 μg mL^{-1}	[96]
Hepatitis B surface antigen (HbsAg)		DPV	Cu-MOF/NH_2/antibody	1 ng mL^{-1} -500 ng mL^{-1}	730 pg mL^{-1}	[131]
Hepatitis B surface antigen (HBsAg), HBsAg, *Anti*-HBs and *Anti*-HBc	Screen printing LFA	EIS Colorimetric	BSA/*anti*-HBsAg Ag/AuNPs-antibody	5–3000 ng mL^{-1} Not specified	2.1 ng mL^{-1} 0.5, 0.3 and 0.1 μg mL^{-1}	[132]
Hepatitis B surface antigen (HbsAg)	Screen printing	DPV	rGO/PB-Au@PtNPs/antibody	0.25–400 ng mL^{-1}	0.08 pg mL^{-1}	[138]
S1 and S2 parts of SARS-CoV-2 S spike glycoproteins	Screen printing	DPV	GO-8H-EDC–NHS–Au NS	Not specified	1.68×10^{-22} μg mL^{-1}	[182]

Table 2
Summary of nucleic acid-based PADs for virus sensing.

Target	Fabrication Method	Detection Method	Label/Biorecognition element	Linear Range	LOD	Ref.
influenza virus H1N1 RNA	LFA	Fluorescence	fluorescent nanospheres (FNs)-DNA/ streptaividin-biotin	Not specified	2.02 pM	[148]
zika, dengue, and chikungunya virus RNA	LFA	Fluorescence	Chitosan/hydroxylnaphthol blue (HNB)	5 -5000 copies zika virus	Not specified	[151]
Target DNA	LFA	Colorimetric	Chitosan/5′-digoxigenin- and 3′-biotin-labeled oligonucleotide probe	Not specified	1.16×10^{-15} mol	[152]
GII.4 and GII.17 genotypes of norovirus	Cutting	Colorimetric	Chlorophenol red-β-D-galactopyranoside (CPRG)/β-galactosidase/RNA-based riboswitch	Not specified	0.5 pM and 2.6 fM	[153]
respiratory syncytial virus subgroups A and B	Cutting	Colorimetric	Chlorophenol red-β-D-galactopyranoside (CPRG)/β-galactosidase/RNA-based riboswitch	Not specified	52 aM and 91 aM	[154]
hantavirus (HTNV), chikungunya fever virus (CHIKV), dengue virus (DENV), and Ebola virus (EBOV)	LFA	Colorimetric	AuNPs/capture probe/magnetic beads	Not specified	10 fM	[156]
SARS-CoV-2 N2 gene IVT RNA	LFA	Colorimetric	Cas12 gRNAs/FAM-biotinylated reporter molecule	Not specified	10 copies/μL	[161]
Norovirus DNA	screen-printing and Wax printing	DPV	Ox-g-C_3N_4 NPs	Not specified	100 fM	[171]
DENV 1,2,3,4 DNAs	Stencil printing	CV	GO-SiO_2 nanocomposite	100 pM −1.0 μM	100 pM	[173]
SARS-CoV-2 RNA	Screen printing	DPV	Au@SCX8-RGO-TB-LP-AP and target-HT-CP-Au@Fe_3O_4 sandwich format	10^{-17} and 10^{-12} M	200 copies mL^{-1}	[175]
HIV DNA	Vacuum filtration/ cutting	DPV	Ni—Au composite/CNT/PVA	10 nM-1 μM	0.13 nM	[177]
HBV DNA	Wax printing, screen printing, LFA	ASWV	acpcPNA probe/Au^{3+}	10 pM-2 μM	7.23 pM	[185]

applied to collect A-apt/RGNNV-CP/C-apt-biotin—streptavidin MBs complex, followed by performing the SDA reaction via Nt.BbvCI enzyme at 37°C for 30 min. After the amplification reaction, the produced single-stranded DNA (ssDNA) was introduced to the sample pad. Then, they were captured by AuNPs-DNA conjugates due to the complementary reaction in the presence of the RGNNV-CP. The red color was visually observed in 5 min and the LOD was 5 ng mL^{-1} for RGNNV-CP. This work is the first sensing platform for virus detection in aquaculture, which combines LFA and aptamer. The developed PAD has an advantage that RNA extraction and purification steps are not necessary. Another aptamer-based PAD was developed by for p24-HIV protein detection [190]. Graphene quantum dots were produced and used to modify screen-printed electrode surface via electrodeposition by CV. Then, the aptamer was immobilized via EDC/NHS coupling due to the formation of a covalent bond between the carboxylic groups of GQDs and the amino group of the aptamer. BSA was used to block nonspecific sites on the electrode surface, followed by label-free detection of p24-HIV due to the decrease in the electrochemical probe anodic peak current using. The LOD obtained was 51.7 pg mL^{-1} with a linear range from 0.93 ng mL^{-1} to 93 mg mL^{-1} using CV. The aptasensor was stable for four weeks.

All discussed articles were summarized in Table 1 and Table 2 with the detection technique, recognition element/assay, working linear range and LOD of the PADs.

5. Conclusions and future prospects

In this review, the current state-of-the-art approaches for electrochemical and optical-based PADs for detection of viruses were described based on the bio-recognition elements including nucleic acids, antibodies, antigens, aptamers, and peptide nucleic acids used to provide selectivity. We also specifically highlighted work that addressed the COVID-19 pandemic as well.

Paper has many advantages for virus detection including its capability to store active biomolecules for long periods, pump free flow, and low-cost. Among the many applications, colorimetric LFAs for virus detection have become common with improved sensitivity and specificity owing to recent improvements in both labels and flow control. Among aforementioned colorimetric LFAs based on antibody as a recognition element, the immunosensor developed by Adrover-Jaume et al. for detection of IL-6 is promising as POC diagnosis for future viral diseases due to its applications in blood and respiratory samples from COVID-19 patients and fast response time (less than 10 min) [118]. However, LOD could be further improved and stability studies should be performed to be used in possible pandemics in the future. Although antibodies are widely used incorporation with LFAs for viral detection, they have disadvantages compared to nucleic acids due to their high-cost of production, low stability, and potential for cross-reactivity with other diseases. Emerging technologies like CRISPR along with isothermal amplification methods will pave the way for POC detection of viral nucleic acids, providing an alternative for future pandemics as well as addressing on-going needs in common infectious diseases. The LFA developed for detection of SARS-CoV-2 using CRISPR technology by Broughton et al. can be adapted for sensitive detection of future pandemics [161] due to its successful application in clinical samples. In addition, molecular imprinting strategies that mimic the interaction between antibodies and antigens has been recently used for the detection of viruses [191]. However, virus size, variability in structure, and low stability in organic solvents may limit applications. “Monoclonal-type” plastic antibodies based on molecularly imprinted polymers (MIPs) were demonstrated by Parisi et al. for selective detection of SARS-CoV-2 spike protein [192].

Although PADs are often successfully analyzed in either buffered solutions or real samples spiked with target viruses, the performance can be adversely affected by complex sample matrixes. The limitations in the stability and accuracy of ePADs may be overcome with the application of nanomaterials and various antifouling layers such as polyethylene glycol, zwitterionic polymers, synthetic peptides, and carbon nanomaterials. In addition,

PNAs hold great promise for electrochemical sensing platforms due to their low detection limits, typically in the attomolar range, and stability against high ionic strength and temperature. In aforementioned study carried out by Srisomwat et al., PNA as recognition element for label-free HPV detection strategy could be useful for future viruses as well [77]. Moreover, aptamers should be exploited for simultaneous detection of viruses by immobilizing multiple aptamers on a single device. The aptamer-based electrochemical PAD developed for p24-HIV protein detection is promising to detect viruses in the future due its low LOD and long stability (four weeks), which is crucial for distribution of the detection kits worldwide during pandemics [190]. However, this biosensor requires a portable read-out device for electrochemical detection. To tackle with this issue, wireless and portable NFC-Potentiostat has been introduced by the Henry and Chailapakul group [96].

In the future, machine learning and artificial intelligence (AI) approaches with wireless communication will be trending for viral sensing, enabling rapid transfer of analysis results to decision makers in hospitals [193]. Besides, timely decision in viral diagnostics could be achieved by AI-supported sensing strategies along with IoT and bioinformatics-based big data analysis. In this context, significant efforts have been made for COVID-19 management [194,195].

Declaration of competing interest

The authors declare that they have no known competing financial interests or personal relationships that could have appeared to influence the work reported in this paper.

Acknowledgment

This work was supported by bilateral grant funded by the research program of The Scientific and Technological Research Council of Turkey and the National Science and Technology Development Agency of Thailand (No.120N615). Additional support was provided by the US National Science Foundation (CHEM-1710222) and the US National Institutes of Health (R21EB030349).

References

[1] B.M. Davis, G.F. Rall, M.J. Schnell, Everything you always wanted to know about rabies virus (but were afraid to ask), Annual review of virology 2 (2015) 451–471.
[2] C. da Cruz Santos, et al., A new tool for dengue virus diagnosis: optimization and detection of anti-NS1 antibodies in serum samples by impedimetric transducers, Microchem. J. 154 (2020) 104544.
[3] R.H. Purcell, Hepatitis viruses: changing patterns of human disease, Proc. Natl. Acad. Sci. Unit. States Am. 91 (7) (1994) 2401–2406.
[4] E.C. Holmes, et al., The evolution of Ebola virus: insights from the 2013–2016 epidemic, Nature 538 (7624) (2016) 193–200.
[5] Y.N. Vaishnav, F. Wong-Staal, The biochemistry of AIDS, Annu. Rev. Biochem. 60 (1) (1991) 577–630.
[6] D.-H. Lee, M.F. Criado, D.E. Swayne, Pathobiological origins and evolutionary history of highly pathogenic avian influenza viruses, Cold Spring Harbor perspectives in medicine 11 (2) (2021) a038679.
[7] V.G. da Costa, M.L. Moreli, M.V. Saivish, The emergence of SARS, MERS and novel SARS-2 coronaviruses in the 21st century, Arch. Virol. 165 (7) (2020) 1517–1526.
[8] E. Vermisoglou, et al., Human virus detection with graphene-based materials, Biosens. Bioelectron. 166 (2020) 112436.
[9] Z. Liu, et al., Disease burden of viral hepatitis A, B, C and E: a systematic analysis, J. Viral Hepat. 27 (12) (2020) 1284–1296.
[10] N. Castaño, et al., Fomite transmission, physicochemical origin of virus–surface interactions, and disinfection strategies for enveloped viruses with applications to SARS-CoV-2, ACS Omega 6 (10) (2021) 6509–6527.
[11] T. Ozer, B.J. Geiss, C.S. Henry, Chemical and biological sensors for viral detection, J. Electrochem. Soc. 167 (3) (2019) 37523.
[12] M. Moriyama, W.J. Hugentobler, A. Iwasaki, Seasonality of respiratory viral infections, Annual review of virology 7 (2020) 83–101.
[13] Y. Rasmi, et al., Emerging point-of-care biosensors for rapid diagnosis of COVID-19: current progress, challenges, and future prospects, Anal. Bioanal. Chem. (2021) 1–23.
[14] G.E. Greening, J.L. Cannon, Human and animal viruses in food (including taxonomy of enteric viruses), in: Viruses in Foods, Springer, 2016, pp. 5–57.
[15] O. Pashchenko, et al., A comparison of optical, electrochemical, magnetic, and colorimetric point-of-care biosensors for infectious disease diagnosis, ACS Infect. Dis. 4 (8) (2018) 1162–1178.
[16] D. DiMaio, L.W. Enquist, T.S. Dermody, A new coronavirus emerges, this time causing a pandemic, Annual review of virology 7 (2020). iii–v.
[17] A. Siddharta, et al., Virucidal activity of World Health Organization–recommended formulations against enveloped viruses, including Zika, Ebola, and emerging coronaviruses, J. Infect. Dis. 215 (6) (2017) 902–906.
[18] C.c. Ménard-Moyon, A. Bianco, K. Kalantar-Zadeh, Two-dimensional material-based biosensors for virus detection, ACS Sens. 5 (12) (2020) 3739–3769.
[19] A. Krishnan, et al., A narrative review of coronavirus disease 2019 (COVID-19): clinical, epidemiological characteristics, and systemic manifestations, Internal and Emergency Medicine (2021) 1–16.
[20] A. Spinelli, G. Pellino, COVID-19 pandemic: perspectives on an unfolding crisis, J British Surg 107 (7) (2020) 785–787.
[21] M. Monajjemi, S. Shahriari, F. Mollaamin, Evaluation of Coronavirus families & Covid-19 proteins: molecular modeling study, Biointerface Res. Appl. Chem 10 (2020) 6039–6057.
[22] Z.Y. Zu, et al., Coronavirus disease 2019 (COVID-19): a perspective from China, Radiology 296 (2) (2020) E15–E25.
[23] P. Zhou, et al., A pneumonia outbreak associated with a new coronavirus of probable bat origin, Nature 579 (7798) (2020) 270–273.
[24] W. Tai, et al., Characterization of the receptor-binding domain (RBD) of protein as a viral attachment inhibitor and vaccine, Cell. Mol. Immunol. 17 (2020) 613–620.
[25] B. Alhalaili, et al., Nanobiosensors for the detection of novel coronavirus 2019-nCoV and other pandemic/epidemic respiratory viruses: a review, Sensors 20 (22) (2020) 6591.
[26] R.M. Torrente-Rodríguez, et al., SARS-CoV-2 RapidPlex: a graphene-based multiplexed telemedicine platform for rapid and low-cost COVID-19 diagnosis and monitoring, Matter 3 (6) (2020) 1981–1998.
[27] H.-Y. Li, et al., Advances in detection of infectious agents by aptamer-based technologies, Emerg. Microb. Infect. 9 (1) (2020) 1671–1681.
[28] M.A. El-Mokhtar, et al., Hepatitis C virus affects tuberculosis-specific T cells in HIV-negative patients, Viruses 12 (1) (2020) 101.
[29] A. Bandera, et al., Phylogenies in ART: HIV reservoirs, HIV latency and drug resistance, Curr. Opin. Pharmacol. 48 (2019) 24–32.
[30] S.H. Baek, et al., Development of a rapid and sensitive electrochemical biosensor for detection of human norovirus via novel specific binding peptides, Biosens. Bioelectron. 123 (2019) 223–229.
[31] R.L. Atmar, S. Ramani, M.K. Estes, Human noroviruses: recent advances in a 50-year history, Curr. Opin. Infect. Dis. 31 (5) (2018) 422–432.
[32] A.R. Falsey, et al., Respiratory syncytial virus infection in elderly and high-risk adults, N. Engl. J. Med. 352 (17) (2005) 1749–1759.
[33] J.S. Tregoning, J. Schwarze, Respiratory viral infections in infants: causes, clinical symptoms, virology, and immunology, Clin. Microbiol. Rev. 23 (1) (2010) 74–98.
[34] A.C. Moço, et al., Electrochemical detection of zika virus in biological samples: a step for diagnosis point-of-care, Electroanalysis 31 (8) (2019) 1580–1587.
[35] D. Musso, M.C. Lanteri, Emergence of Zika virus: where does it come from and where is it going to? Lancet Infect. Dis. 17 (3) (2017) 255.
[36] A. George, et al., Label-free detection of Chikungunya non-structural protein 3 using electrochemical impedance spectroscopy, J. Electrochem. Soc. 166 (14) (2019) B1356.
[37] W.H. Organization, Chikungunya Fact Sheet, World Health Organization, Geneva, Switzerland, 2016.
[38] Y.-P. Liu, C.-Y. Yao, Rapid and quantitative detection of hepatitis B virus, World J. Gastroenterol. 21 (42) (2015) 11954.
[39] T.J. Liang, Hepatitis B: the virus and disease, Hepatology 49 (S5) (2009) S13–S21.
[40] W. Xiao, et al., A simple and compact smartphone-based device for the quantitative readout of colloidal gold lateral flow immunoassay strips, Sensor. Actuator. B Chem. 266 (2018) 63–70.
[41] S. Fan, et al., Pseudorabies virus encephalitis in humans: a case series study, J. Neurovirol. 26 (4) (2020) 556–564.
[42] J.-W. Ai, et al., Human endophthalmitis caused by pseudorabies virus infection, China, 2017, Emerg. Infect. Dis. 24 (6) (2018) 1087.
[43] H. Zhu, et al., Recent advances in lab-on-a-chip technologies for viral diagnosis, Biosens. Bioelectron. 153 (2020) 112041.
[44] L.A. Bastian, et al., Diagnostic efficiency of home pregnancy test kits: a meta-analysis, Arch. Fam. Med. 7 (5) (1998) 465.
[45] T. Ozer, C. McMahon, C.S. Henry, Advances in paper-based analytical devices, Annu. Rev. Anal. Chem. 13 (2020) 85–109.
[46] A.W. Martinez, et al., Patterned paper as a platform for inexpensive, low-volume, portable bioassays, Angew. Chem. 119 (8) (2007) 1340–1342.
[47] E. Carrilho, A.W. Martinez, G.M. Whitesides, Understanding wax printing: a simple micropatterning process for paper-based microfluidics, Anal. Chem. 81 (16) (2009) 7091–7095.

[48] W. Dungchai, O. Chailapakul, C.S. Henry, Electrochemical detection for paper-based microfluidics, Anal. Chem. 81 (14) (2009) 5821–5826.
[49] V.N. Ataide, et al., Electrochemical paper-based analytical devices: ten years of development, Analytical Methods 12 (8) (2020) 1030–1054.
[50] M.C. Barr, et al., Direct monolithic integration of organic photovoltaic circuits on unmodified paper, Adv. Mater. 23 (31) (2011) 3500–3505.
[51] A. Apilux, et al., Lab-on-paper with dual electrochemical/colorimetric detection for simultaneous determination of gold and iron, Anal. Chem. 82 (5) (2010) 1727–1732.
[52] E. Solhi, M. Hasanzadeh, P. Babaie, Electrochemical paper-based analytical devices (ePADs) toward biosensing: recent advances and challenges in bioanalysis, Analytical Methods 12 (11) (2020) 1398–1414.
[53] S. Kasetsirikul, M.J. Shiddiky, N.-T. Nguyen, Challenges and perspectives in the development of paper-based lateral flow assays, Microfluid. Nanofluidics 24 (2) (2020) 1–18.
[54] L.-M. Fu, Y.-N. Wang, Detection methods and applications of microfluidic paper-based analytical devices, Trac. Trends Anal. Chem. 107 (2018) 196–211.
[55] K. Abe, et al., Inkjet-printed paperfluidic immuno-chemical sensing device, Anal. Bioanal. Chem. 398 (2) (2010) 885–893.
[56] J. Olkkonen, K. Lehtinen, T. Erho, Flexographically printed fluidic structures in paper, Anal. Chem. 82 (24) (2010) 10246–10250.
[57] X. Li, et al., Based microfluidic devices by plasma treatment, Anal. Chem. 80 (23) (2008) 9131–9134.
[58] G. Chitnis, et al., Laser-treated hydrophobic paper: an inexpensive microfluidic platform, Lab Chip 11 (6) (2011) 1161–1165.
[59] Q. He, et al., Method for fabrication of paper-based microfluidic devices by alkylsilane self-assembling and UV/O3-patterning, Anal. Chem. 85 (3) (2013) 1327–1331.
[60] P. de Tarso Garcia, G. Cardoso, Tm, C.D. Garcia, E. Carrilho, W.K. Tomazelli Coltro, A handheld stamping process to fabricate microfluidic paper-based analytical devices with chemically modified surface for clinical assays, RSC Adv. 4 (71) (2014) 37637–37644.
[61] T. Nurak, N. Praphairaksit, O. Chailapakul, Fabrication of paper-based devices by lacquer spraying method for the determination of nickel (II) ion in waste water, Talanta 114 (2013) 291–296.
[62] Y. Sameenoi, et al., One-step polymer screen-printing for microfluidic paper-based analytical device (μPAD) fabrication, Analyst 139 (24) (2014) 6580–6588.
[63] N. Nuchtavorn, M. Macka, A novel highly flexible, simple, rapid and low-cost fabrication tool for paper-based microfluidic devices (μPADs) using technical drawing pens and in-house formulated aqueous inks, Anal. Chim. Acta 919 (2016) 70–77.
[64] W. Suntornsuk, L. Suntornsuk, Recent applications of paper-based point-of-care devices for biomarker detection, Electrophoresis 41 (5–6) (2020) 287–305.
[65] C. Carrell, et al., Beyond the lateral flow assay: a review of paper-based microfluidics, Microelectron. Eng. 206 (2019) 45–54.
[66] M. Sajid, A.-N. Kawde, M. Daud, Designs, formats and applications of lateral flow assay: a literature review, J. Saudi Chem. Society 19 (6) (2015) 689–705.
[67] J.-H. Lee, et al., Multiplex diagnosis of viral infectious diseases (AIDS, hepatitis C, and hepatitis A) based on point of care lateral flow assay using engineered proteinticles, Biosens. Bioelectron. 69 (2015) 213–225.
[68] D. Duan, et al., Nanozyme-strip for rapid local diagnosis of Ebola, Biosens. Bioelectron. 74 (2015) 134–141.
[69] T. Salminen, et al., Anti-HCV immunoassays based on a multiepitope antigen and fluorescent lanthanide chelate reporters, J. Virol Methods 228 (2016) 67–73.
[70] J. Shen, et al., Immunochromatographic assay for quantitative and sensitive detection of hepatitis B virus surface antigen using highly luminescent quantum dot-beads, Talanta 142 (2015) 145–149.
[71] W. Qiu, et al., Carbon nanotube-based lateral flow biosensor for sensitive and rapid detection of DNA sequence, Biosens. Bioelectron. 64 (2015) 367–372.
[72] K.-K. Fung, C.P.-Y. Chan, R. Renneberg, Development of enzyme-based bar code-style lateral-flow assay for hydrogen peroxide determination, Anal. Chim. Acta 634 (1) (2009) 89–95.
[73] K.A. Edwards, A.J. Baeumner, Optimization of DNA-tagged dye-encapsulating liposomes for lateral-flow assays based on sandwich hybridization, Anal. Bioanal. Chem. 386 (5) (2006) 1335–1343.
[74] R. Wong, H. Tse, Lateral Flow Immunoassay, Springer Science & Business Media, 2008.
[75] M.A. Black, et al., Analytical performance of lateral flow immunoassay for SARS-CoV-2 exposure screening on venous and capillary blood samples, J. Immunol. Methods 489 (2021) 112909.
[76] A.W. Martinez, et al., Programmable diagnostic devices made from paper and tape, Lab Chip 10 (19) (2010) 2499–2504.
[77] C. Srisomwat, et al., Pop-up paper electrochemical device for label-free hepatitis B virus DNA detection, Sensor. Actuator. B Chem. 316 (2020) 128077.
[78] C.-A. Chen, et al., An electricity-and instrument-free infectious disease sensor based on a 3D origami paper-based analytical device, Lab Chip 21 (10) (2021) 1908–1915.
[79] E. Noviana, et al., Electrochemical paper-based devices: sensing approaches and progress toward practical applications, Lab Chip 20 (1) (2019) 9–34.
[80] E. Noviana, C.S. Henry, Simultaneous electrochemical detection in paper-based analytical devices, Current Opinion in Electrochem. 23 (2020) 1–6.
[81] E. Noviana, et al., Microfluidic paper-based analytical devices: from design to applications, Chem. Rev. (2021). https://doi.org/10.1021/acs.chemrev.0c01335.
[82] S.K. Bhardwaj, et al., Recent progress in nanomaterial-based sensing of airborne viral and bacterial pathogens, Environ. Int. 146 (2021) 106183.
[83] D.M. Cate, et al., Simple, distance-based measurement for paper analytical devices, Lab Chip 13 (12) (2013) 2397–2404.
[84] L.P. Murray, C.R. Mace, Usability as a guiding principle for the design of paper-based, point-of-care devices—A Review, Anal. Chim. Acta 1140 (2020) 236–249.
[85] J. Zhuang, et al., Advanced “lab-on-a-chip” to detect viruses—Current challenges and future perspectives, Biosens. Bioelectron. (2020) 112291.
[86] R.R.X. Lim, A. Bonanni, The potential of electrochemistry for the detection of coronavirus-induced infections, Trac. Trends Anal. Chem. 133 (2020) 116081.
[87] S. Menon, et al., Recent advances and challenges in electrochemical biosensors for emerging and re-emerging infectious diseases, J. Electroanal. Chem. (2020) 114596.
[88] H.S. Maghded, et al., A novel AI-enabled framework to diagnose coronavirus COVID-19 using smartphone embedded sensors: design study, in: 2020 IEEE 21st International Conference on Information Reuse and Integration for Data Science (IRI), IEEE, 2020.
[89] W. Chen, et al., Application of smartphone-based spectroscopy to biosample analysis: a review, Biosens. Bioelectron. (2020) 112788.
[90] S. Banik, et al., Recent trends in smartphone-based detection for biomedical applications: a review, Anal. Bioanal. Chem. (2021) 1–18.
[91] A. Ozcan, Mobile phones democratize and cultivate next-generation imaging, diagnostics and measurement tools, Lab Chip 14 (17) (2014) 3187–3194.
[92] Y. Rivenson, et al., Deep learning enhanced mobile-phone microscopy, ACS Photonics 5 (6) (2018) 2354–2364.
[93] S. Olenik, H.S. Lee, F. Güder, The future of near-field communication-based wireless sensing, Nature Reviews Materials (2021) 1–3.
[94] J. Nelis, et al., Smartphone-based optical assays in the food safety field, Trac. Trends Anal. Chem. 129 (2020) 115934.
[95] B. Hunt, A.J. Ruiz, B.W. Pogue, Smartphone-based imaging systems for medical applications: a critical review, J. Biomed. Opt. 26 (4) (2021) 40902.
[96] P. Teengam, et al., NFC-enabling smartphone-based portable amperometric immunosensor for hepatitis B virus detection, Sensor. Actuator. B Chem. 326 (2021) 128825.
[97] B. Lakard, Electrochemical biosensors based on conducting polymers: a review, Appl. Sci. 10 (18) (2020) 6614.
[98] S.A. Lim, M.U. Ahmed, Introduction to Immunosensors, 2019.
[99] E. Boel, et al., Functional human monoclonal antibodies of all isotypes constructed from phage display library-derived single-chain Fv antibody fragments, J. Immunol. Methods 239 (1–2) (2000) 153–166.
[100] N.S. Lipman, et al., Monoclonal versus polyclonal antibodies: distinguishing characteristics, applications, and information resources, ILAR J. 46 (3) (2005) 258–268.
[101] S.A. Abid, et al., Biosensors as a Future Diagnostic Approach for COVID-19, Life Sciences, 2021, p. 119117.
[102] F. Zhang, et al., Single chain fragment variable (scFv) antibodies targeting the spike protein of porcine epidemic diarrhea virus provide protection against viral infection in piglets, Viruses 11 (1) (2019) 58.
[103] S. Sharma, H. Byrne, R.J. O'Kennedy, Antibodies and antibody-derived analytical biosensors, Essays Biochem. 60 (1) (2016) 9–18.
[104] I. Migneault, et al., Glutaraldehyde: behavior in aqueous solution, reaction with proteins, and application to enzyme crosslinking, Biotechniques 37 (5) (2004) 790–802.
[105] M.J. Fischer, Amine coupling through EDC/NHS: a practical approach, in: Surface Plasmon Resonance, Springer, 2010, pp. 55–73.
[106] A.A. Karyakin, et al., Oriented immobilization of antibodies onto the gold surfaces via their native thiol groups, Anal. Chem. 72 (16) (2000) 3805–3811.
[107] Z. Grabarek, J. Gergely, Zero-length crosslinking procedure with the use of active esters, Anal. Biochem. 185 (1) (1990) 131–135.
[108] N.G. Welch, et al., Orientation and characterization of immobilized antibodies for improved immunoassays, Biointerphases 12 (2) (2017), 02D301.
[109] S.K. Vashist, J.H. Luong, Antibody immobilization and surface functionalization chemistries for immunodiagnostics, in: Handbook of Immunoassay Technologies, Elsevier, 2018, pp. 19–46.
[110] Z. You, et al., Laser-induced noble metal nanoparticle-graphene composites enabled flexible biosensor for pathogen detection, Biosens. Bioelectron. 150 (2020) 111896.
[111] H. Cui, et al., Simultaneous and sensitive detection of dual DNA targets via quantum dot-assembled amplification labels, Luminescence 31 (1) (2016) 281–287.
[112] T. Liao, et al., Lanthanide chelate-encapsulated polystyrene nanoparticles for rapid and quantitative immunochromatographic assay of procalcitonin, RSC Adv. 6 (105) (2016) 103463–103470.
[113] Z. Chen, et al., Rapid and sensitive detection of anti-SARS-CoV-2 IgG, using lanthanide-doped nanoparticles-based lateral flow immunoassay, Anal. Chem. 92 (10) (2020) 7226–7231.
[114] H. Jung, et al., A size-selectively biomolecule-immobilized nanoprobe-based chemiluminescent lateral flow immunoassay for detection of avian-origin viruses, Anal. Chem. 93 (2) (2020) 792–800.

[115] L. Huang, et al., Miniaturized paper-based smartphone biosensor for differential diagnosis of wild-type pseudorabies virus infection versus vaccination immunization, Sensor. Actuator. B Chem. 327 (2021) 128893.
[116] H. Han, et al., Profiling serum cytokines in COVID-19 patients reveals IL-6 and IL-10 are disease severity predictors, Emerg. Microb. Infect. 9 (1) (2020) 1123–1130.
[117] J.-S. Kwon, et al., Factors of severity in patients with COVID-19: cytokine/chemokine concentrations, viral load, and antibody responses, Am. J. Trop. Med. Hyg. 103 (6) (2020) 2412–2418.
[118] C. Adrover-Jaume, et al., Paper biosensors for detecting elevated IL-6 levels in blood and respiratory samples from COVID-19 patients, Sensor. Actuator. B Chem. 330 (2021) 129333.
[119] S. Di, et al., Recent advances and applications of magnetic nanomaterials in environmental sample analysis, Trac. Trends Anal. Chem. 126 (2020) 115864.
[120] A. Waheed, M. Mansha, N. Ullah, Nanomaterials-based electrochemical detection of heavy metals in water: current status, challenges and future direction, Trac. Trends Anal. Chem. 105 (2018) 37–51.
[121] V. Georgakilas, et al., Broad family of carbon nanoallotropes: classification, chemistry, and applications of fullerenes, carbon dots, nanotubes, graphene, nanodiamonds, and combined superstructures, Chem. Rev. 115 (11) (2015) 4744–4822.
[122] J. Kim, S.-J. Park, D.-H. Min, Emerging approaches for graphene oxide biosensor, Anal. Chem. 89 (1) (2017) 232–248.
[123] C. Chung, et al., Biomedical applications of graphene and graphene oxide, Acc. Chem. Res. 46 (10) (2013) 2211–2224.
[124] A. Yakoh, et al., Based electrochemical biosensor for diagnosing COVID-19: detection of SARS-CoV-2 antibodies and antigen, Biosens. Bioelectron. 176 (2021) 112912.
[125] S. Eissa, M. Zourob, Development of a low-cost cotton-tipped electrochemical immunosensor for the detection of SARS-CoV-2, Anal. Chem. 93 (3) (2020) 1826–1833.
[126] M.S. Wilson, Electrochemical immunosensors for the simultaneous detection of two tumor markers, Anal. Chem. 77 (5) (2005) 1496–1502.
[127] F. Mollarasouli, et al., Magnetic nanoparticles in developing electrochemical sensors for pharmaceutical and biomedical applications, Talanta 226 (2021) 122108.
[128] L. Fabiani, et al., Magnetic beads combined with carbon black-based screen-printed electrodes for COVID-19: a reliable and miniaturized electrochemical immunosensor for SARS-CoV-2 detection in saliva, Biosens. Bioelectron. 171 (2021) 112686.
[129] P. Kassal, M.D. Steinberg, I.M. Steinberg, Wireless chemical sensors and biosensors: a review, Sensor. Actuator. B Chem. 266 (2018) 228–245.
[130] V. Coskun, B. Ozdenizci, K. Ok, A survey on near field communication (NFC) technology, Wireless Pers. Commun. 71 (3) (2013) 2259–2294.
[131] M. Rezki, et al., Amine-functionalized Cu-MOF nanospheres towards label-free hepatitis B surface antigen electrochemical immunosensors, J. Mater. Chem. B 9 (2021) 5711–5721.
[132] C. Akkapinyo, et al., Development of a multiplex immunochromatographic strip test and ultrasensitive electrochemical immunosensor for hepatitis B virus screening, Anal. Chim. Acta 1095 (2020) 162–171.
[133] M. Krajden, G. McNabb, M. Petric, The laboratory diagnosis of hepatitis B virus, Can. J. Infect Dis. Med. Microbiol. 16 (2) (2005) 65–72.
[134] J.-H. Kao, Diagnosis of hepatitis B virus infection through serological and virological markers, Expet Rev. Gastroenterol. Hepatol. 2 (4) (2008) 553–562.
[135] Z. Zhao, et al., Advancements in electrochemical biosensing for respiratory virus detection: a review, Trac. Trends Anal. Chem. 139 (2021) 116253.
[136] X. Li, et al., Development of a novel label-free impedimetric electrochemical sensor based on hydrogel/chitosan for the detection of ochratoxin A, Talanta 226 (2021) 122183.
[137] E. Cesewski, B.N. Johnson, Electrochemical biosensors for pathogen detection, Biosens. Bioelectron. (2020) 112214.
[138] S. Wei, et al., Ultrasensitive label-free electrochemical immunosensor based on core-shell Au@ PtNPs functionalized rGO-TEPA/PB nanocomposite for HBsAg detection, J. Electroanal. Chem. 890 (2021) 115216.
[139] M. Baker, Antibody anarchy: a call to order, Nature 527 (7579) (2015) 545–551.
[140] R. O'Kennedy, S. Fitzgerald, C. Murphy, Don't blame it all on antibodies—The need for exhaustive characterisation, appropriate handling, and addressing the issues that affect specificity, Trac. Trends Anal. Chem. 89 (2017) 53–59.
[141] D.C. Benjamin, S.S. Perdue, Site-directed mutagenesis in epitope mapping, Methods 9 (3) (1996) 508–515.
[142] G. Seo, et al., Rapid detection of COVID-19 causative virus (SARS-CoV-2) in human nasopharyngeal swab specimens using field-effect transistor-based biosensor, ACS Nano 14 (4) (2020) 5135–5142.
[143] M. Pividori, A. Merkoci, S. Alegret, Electrochemical genosensor design: immobilisation of oligonucleotides onto transducer surfaces and detection methods, Biosens. Bioelectron. 15 (5–6) (2000) 291–303.
[144] W. Su, D. Liang, M. Tan, Nucleic acid-based detection for foodborne virus utilizing microfluidic systems, Trends Food Sci. Technol. 113 (2021) 97–109.
[145] A. Suea-Ngam, et al., Enzyme-assisted nucleic acid detection for infectious disease diagnostics: moving toward the point-of-care, ACS Sens. 5 (9) (2020) 2701–2723.
[146] Z.-y. Wang, et al., Integration of nanomaterials with nucleic acid amplification approaches for biosensing, Trac. Trends Anal. Chem. 129 (2020) 115959.
[147] L. Xu, et al., Recent advances in rolling circle amplification-based biosensing strategies-A review, Anal. Chim. Acta 1148 (2020) 23818.
[148] S. Li, et al., Entropy-driven amplification strategy-assisted lateral flow assay biosensor for ultrasensitive and convenient detection of nucleic acids, Analyst 146 (5) (2021) 1668–1674.
[149] J.T. Connelly, J.P. Rolland, G.M. Whitesides, "Paper machine" for molecular diagnostics, Anal. Chem. 87 (15) (2015) 7595–7601.
[150] H. Zhang, et al., LAMP-on-a-chip: revising microfluidic platforms for loop-mediated DNA amplification, Trac. Trends Anal. Chem. 113 (2019) 44–53.
[151] Y. Seok, B.S. Batule, M.-G. Kim, Lab-on-paper for all-in-one molecular diagnostics (LAMDA) of zika, dengue, and chikungunya virus from human serum, Biosens. Bioelectron. 165 (2020) 112400.
[152] E. Noviana, et al., Based nuclease protection assay with on-chip sample pretreatment for point-of-need nucleic acid detection, Anal. Bioanal. Chem. (2020) 1–11.
[153] Q. Sun, et al., A simple and low-cost paper-based colorimetric method for detecting and distinguishing the GII. 4 and GII. 17 genotypes of norovirus, Talanta 225 (2021) 121978.
[154] M. Cao, et al., Detection and differentiation of respiratory syncytial virus subgroups A and B with colorimetric toehold switch sensors in a paper-based cell-free system, Biosens. Bioelectron. 182 (2021) 113173.
[155] B.J. Toley, et al., Isothermal strand displacement amplification (iSDA): a rapid and sensitive method of nucleic acid amplification for point-of-care diagnosis, Analyst 140 (22) (2015) 7540–7549.
[156] J. Zhao, et al., A lateral flow biosensor based on gold nanoparticles detects four hemorrhagic fever viruses, Analytical Methods 12 (46) (2020) 5613–5620.
[157] A. Nocker, A.K. Camper, Novel approaches toward preferential detection of viable cells using nucleic acid amplification techniques, FEMS Microbiol. Lett. 291 (2) (2009) 137–142.
[158] K.S. Makarova, et al., Evolutionary classification of CRISPR–Cas systems: a burst of class 2 and derived variants, Nat. Rev. Microbiol. 18 (2) (2020) 67–83.
[159] B.J. Park, et al., Specific detection of influenza A and B viruses by CRISPR-cas12a-based assay, Biosensors 11 (3) (2021) 88.
[160] J.S. Chen, et al., CRISPR-Cas12a target binding unleashes indiscriminate single-stranded DNase activity, Science 360 (6387) (2018) 436–439.
[161] J.P. Broughton, et al., CRISPR–Cas12-based detection of SARS-CoV-2, Nat. Biotechnol. 38 (7) (2020) 870–874.
[162] H. Rahimi, et al., CRISPR systems for COVID-19 diagnosis, ACS Sens. 6 (4) (2021) 1430–1445.
[163] R. Aman, A. Mahas, M. Mahfouz, Nucleic acid detection using CRISPR/Cas biosensing technologies, ACS Synth. Biol. 9 (6) (2020) 1226–1233.
[164] M. Wang, R. Zhang, J. Li, CRISPR/cas Systems Redefine Nucleic Acid Detection: Principles and Methods, Biosensors and Bioelectronics, 2020, p. 112430.
[165] J.E. van Dongen, et al., Point-of-care CRISPR/Cas nucleic acid detection: recent advances, challenges and opportunities, Biosens. Bioelectron. 166 (2020) 112445.
[166] Y. Saylan, et al., An alternative medical diagnosis method: biosensors for virus detection, Biosensors 9 (2) (2019) 65.
[167] J. Narang, et al., Development of MoSe2 nano-urchins as a sensing platform for a selective bio-capturing of Escherichia coli shiga toxin DNA, Biosensors 8 (3) (2018) 77.
[168] H.L.L. Yu, A. Maslova, I.M. Hsing, Rational design of electrochemical DNA biosensors for Point-of-Care applications, ChemElectroChem 4 (4) (2017) 795–805.
[169] H. Duwensee, et al., Electrochemical product detection of an asymmetric convective polymerase chain reaction, Biosens. Bioelectron. 25 (2) (2009) 400–405.
[170] X. Lu, et al., Real-time reverse transcription-PCR assay panel for Middle East respiratory syndrome coronavirus, J. Clin. Microbiol. 52 (1) (2014) 67–75.
[171] A. Rana, et al., Graphitic carbon nitride as an amplification platform on an electrochemical paper-based device for the detection of norovirus-specific DNA, Sensors 20 (7) (2020) 2070.
[172] H.-J. Niu, et al., Graphene-encapsulated cobalt nanoparticles embedded in porous nitrogen-doped graphitic carbon nanosheets as efficient electrocatalysts for oxygen reduction reaction, J. Colloid Interface Sci. 552 (2019) 744–751.
[173] C. Singhal, et al., Electrochemical multiplexed paper nanosensor for specific dengue serotype detection predicting pervasiveness of DHF/DSS, ACS Biomater. Sci. Eng. 6 (10) (2020) 5886–5894.
[174] M. Lazerges, et al., Electrochemical DNA-biosensors: two-electrode setup well adapted for miniaturized devices, Sensor. Actuator. B Chem. 182 (2013) 510–513.

[175] H. Zhao, et al., Ultrasensitive supersandwich-type electrochemical sensor for SARS-CoV-2 from the infected COVID-19 patients using a smartphone, Sensor. Actuator. B Chem. 327 (2021) 128899.
[176] S.M. Sheta, et al., A novel HCV electrochemical biosensor based on a polyaniline@ Ni-MOF nanocomposite, Dalton Trans. 49 (26) (2020) 8918–8926.
[177] Q. Lu, et al., Flexible paper-based Ni-MOF composite/AuNPs/CNTs film electrode for HIV DNA detection, Biosens. Bioelectron. (2021) 113229.
[178] Y. Wang, et al., Metal-organic frameworks for virus detection, Biosens. Bioelectron. (2020) 112604.
[179] M. Safaei, et al., A review on metal-organic frameworks: synthesis and applications, Trac. Trends Anal. Chem. 118 (2019) 401–425.
[180] C.R. Cole, C.A. Smith, Glycoprotein biochemistry (structure and function)—a vehicle for teaching many aspects of biochemistry and molecular biology, Biochem. Educ. 17 (4) (1989) 179–189.
[181] K. Stavenhagen, R. Plomp, M. Wuhrer, Site-specific protein N-and O-glycosylation analysis by a C18-porous graphitized carbon–liquid chromatography-electrospray ionization mass spectrometry approach using pronase treated glycopeptides, Anal. Chem. 87 (23) (2015) 11691–11699.
[182] S.A. Hashemi, et al., Ultra-sensitive viral glycoprotein detection NanoSystem toward accurate tracing SARS-CoV-2 in biological/non-biological media, Biosens. Bioelectron. 171 (2021) 112731.
[183] M. Egholm, et al., PNA hybridizes to complementary oligonucleotides obeying the Watson–Crick hydrogen-bonding rules, Nature 365 (6446) (1993) 566–568.
[184] V. Demidov, et al., Sequence selective double strand DNA cleavage by peptide nucleic acid (PNA) targeting using nuclease S1, Nucleic Acids Res. 21 (9) (1993) 2103–2107.
[185] C. Srisomwat, et al., Amplification-free DNA sensor for the one-step detection of the hepatitis B virus using an automated paper-based lateral flow electrochemical device, Anal. Chem. 93 (5) (2020) 2879–2887.
[186] M. Moccia, et al., Emerging technologies in the design of peptide nucleic acids (PNAs) based biosensors, Trac. Trends Anal. Chem. 132 (2020) 116062.
[187] J.-F. Wu, et al., A fluorescence sensing platform of theophylline based on the interaction of RNA aptamer with graphene oxide, RSC Adv. 9 (34) (2019) 19813–19818.
[188] L.S. Liu, et al., Recent developments in aptasensors for diagnostic applications, ACS Appl. Mater. Interfaces 13 (8) (2020) 9329–9358.
[189] J. Liu, et al., Development of a novel lateral flow biosensor combined with aptamer-based Isolation: application for rapid detection of grouper nervous necrosis virus, Front. Microbiol. 11 (2020) 886.
[190] J.L. Gogola, et al., Label-free Aptasensor for p24-HIV protein detection based on Graphene Quantum Dots as an electrochemical signal amplifier, Anal. Chim. Acta (2021) 338548.
[191] M. Gast, H. Sobek, B. Mizaikoff, Advances in imprinting strategies for selective virus recognition a review, Trac. Trends Anal. Chem. 114 (2019) 218–232.
[192] F. Puoci, et al., Monoclonal-type" Plastic Antibodies for SARS-CoV-2 Based on Molecularly Imprinted Polymers, BioRxiv, 2020.
[193] T. Ozer, C.S. Henry, Recent advances in sensor arrays for the simultaneous electrochemical detection of multiple analytes, J. Electrochem. Soc. 168 (2021) 057507.
[194] Q.-V. Pham, et al., Artificial Intelligence (AI) and Big Data for Coronavirus (COVID-19) Pandemic: A Survey on the State-Of-The-Arts, 2020.
[195] A.K. Kaushik, et al., Electrochemical SARS-CoV-2 sensing at point-of-care and artificial intelligence for intelligent COVID-19 management, ACS Applied Bio Materials 3 (11) (2020) 7306–7325.